**Economic and Environmental Impacts of Sustainable Agriculture in Practice and at Scale:**

**Evidence From Mexico**

**Joel Ferguson, University of California Berkeley, joel_ferg@berkeley.edu**
**Bram Govaerts, International Maize and Wheat Improvement Center, b.govaerts@cgiar.org**

***Selected Paper prepared for presentation at the 2024 Agricultural & Applied Economics Association Annual Meeting, New Orleans, LA; July 28-30, 2024***

# Economic and Environmental Impacts of Sustainable Agriculture in Practice and at Scale: Evidence from Mexico

Joel Ferguson[1] Bram Govaerts[2]

[1] University of California, Berkeley
[2] International Maize and Wheat Improvement Center

## Introduction

Meeting the food demands of the Earth's growing and increasingly wealthy population without over-exploiting limited natural resources is one of the most pressing global issues. Overcoming this challenge will likely require substantial changes to food systems across the world (Godfray et al., 2010). "Sustainable intensification," producing more output on land already under cultivation while reducing environmental impacts, has been emphasized as necessary for ensuring food security in the coming decades while meeting environmental goals. However, there is widespread disagreement in the scientific literature over the extent to which sustainable intensification provides meaningful environmental or productivity benefits (Godfray, 2015; Loos et al., 2014; Gunton et al., 2016; Mahon et al., 2017). Indeed, it is not obvious that farmers should be able to profitably reduce the environmental impact of their production.

An important facet of the debate is the limited evidence regarding sustainable intensification practices as they are employed by farmers at scale. Cassman and Grassini (2020) note that "[...] there is little research on putting the components together in viable production systems, and in quantifying [sustainable intensification's] potential in terms of both production and environmental performance in farmers' fields rather than small manicured research plots." Gunton et al. (2016) further emphasize the lack of large-scale, long-term studies of the effects of sustainable intensification technologies and the limited selection of sustainability metrics employed. Estimating the value of the environmental and production benefits as well as the cost of adoption, both in terms of inducing diffusion and potential opportunity costs from foregone alternative production methods, is crucial to determining the extent to which sustainable intensification is a viable approach to improving food security and environmental outcomes.

In this paper, we study the impacts of the MasAgro Productor program (henceforth MasAgro[1]), a large-scale agricultural extension effort in Mexico which was implemented beginning in 2012 with technical backing by the International Maize and Wheat Improvement Center (CIMMYT). Notably, MasAgro widely promoted conservation agriculture, a sustainable intensification technique characterized by minimal soil disturbance or zero-tillage, constant soil cover, and crop rotation (Erenstein, 2002). We measure the diffusion of conservation agriculture over time and space induced by MasAgro using detailed geographic data collected by extension technicians and the normalized difference tillage index (NDTI), a satellite imagery-derived proxy for conservation tillage. Variation in the diffusion process allows us to causally identify the effects of conservation agriculture using event studies and related research designs which incorporate additional exogenous variation.

We focus on two sets of outcomes: economic and environmental benefits. To measure the former, we use two data sources. The first is yield and profit data collected from a subset of farms which implement extension-promoted techniques and business-as-usual management on side-by-side plots. The second is a satellite imagery-derived proxy of agricultural productivity, namely the yearly maximum normalized difference vegetation index (NDVI).

The effects of conservation agriculture adoption on profits are not obvious ex-ante. On one hand, we expect farmers to be profit maximizing, which suggests that inducing a change in technology would lower profits. On the other, extension technicians provide information and training on the implementation of conservation agriculture, which may help farmers overcome barriers to adoption. We provide evidence that profits earned under conservation agriculture are larger than under status quo production and similar to profits under other technologies promoted via extension using data

[1]The broader MasAgro program has four compnents: MasAgro Biodiversidad explores the genetic diversity of maize and wheat. MasAgro Maíz develops and promotes the diffusion of novel maize varieties. MasAgro Trigo is a similar program to MasAgro Maíz for wheat. MasAgro Productor is the subject of this study.

from farmer-managed side-by-side demonstration plots. We find that regardless of the technologies employed, extension plots are almost always more profitable, as supported by a test of first order stochastic dominance. Across multiple specifications, our results also suggest that extension plots that employ conservation agriculture are weakly more profitable than extension plots that do not. These results are supported by event study results which show that the arrival of MasAgro extension causes a persistent 0.6% increase in yearly maximum NDVI.

Our analysis of environmental impacts of conservation agriculture focuses on air quality. Recent research has shown that no-till agriculture adoption is associated with reduced fine particulate matter concentration during periods in the year when tillage would take place (Behrer and Lobell, 2022). Conservation agriculture is also generally incompatible with crop residue burning, which has been associated with worse birth outcomes (Rangel and Vogl, 2019), increased infant and general mortality (Pullabhotla et al., 2023; He et al., 2020), and reduced cognitive performance (Graff Zivin et al., 2020; Lai et al., 2022).

To establish an estimate of the value of environmental benefits generated by conservation agriculture, we analyze the effects of its diffusion on $PM_{10}$ concentration and infant mortality in nearby urban localities, geographic units roughly comparable to census block groups in the United States. Our research design combines information on the timing and location of conservation agriculture adoption with exogenous wind variation to causally identify the effect of diffusion on air quality and the number of infant deaths. Intuitively, the design uses deviations from wind patterns to isolate variation in exposure to conservation agriculture, with localities downwind from many plots that adopted conservation agriculture more exposed than when the wind blows in other directions.

We find that adoption of conservation agriculture in a $0.1° \times 0.1°$ grid cell leads to a 1.3% reduction in $PM_{10}$ concentration in downwind localities during the main maize planting and harvest months. These improvements in air quality translate into meaningful health improvements. Our estimates suggest that a locality with mean downwind exposure to conservation agriculture in 2019 experienced a 7% reduction in the number of monthly infant deaths as a result of improved air quality. Using the value of statistical life in Mexico calculated by de Lima (2020) of $211,406 in 2011 USD, this method estimates 11,421.48 estimated deaths averted at a value of $2,414,569,323, over 31 times the program's cost of implementation.

Finally, we explore one of the potential channels for these environmental benefits: agricultural burning. To do so, we combine satellite imagery-derived measures of burning with our measures of conservation agriculture adoption and use two methods to estimate the effects of adoption on agricultural burning. First, we use the imputation event study estimator developed by Borusyak et al. (2021) to assess pre-trends and analyze dynamic treatment effects, finding a slight reduction in monthly agricultural burning that is highly concentrated in the maize planting and harvest months. Second, we use a spatial fixed effects design to allow for very local heterogeneous time trends. Our preferred estimates suggest that the introduction of extension services to $0.1^\circ \times 0.1^\circ$ grid-cells resulted in 10-20% reductions in the number of agricultural fires in a grid-cell as measured by satellite imagery during the pre-planting and post-harvest months.

This paper's main contribution is in providing a causal estimate of the value of an environmental benefit due to conservation agriculture, a topic which has seen limited causal social science research to begin with. In a 2014 review, Pannell et al. (2014) noted that there was little experimental or quasi-experimental evidence of the impacts of conservation agriculture for small-holder farmers in developing countries. Tambo and Mockshell (2018) employ a propensity score matching approach and find that farmers from nine sub-Saharan African countries who adopt conservation have higher total household income. Deines et al. (2019) estimate a small positive yield benefit of conservation tillage in the US corn belt using the causal forest estimator on remote sensed measures of productivity and adoption. Michler et al. (2019) make headway on causal identification by instrumenting for conservation agriculture adoption with a geographically targeted input subsidy program in Zimbabwe. They find that effects on yields are typically negligible, or even negative, except in the presence of exceptional rainfall shocks. A small experimental literature has studied particular interventions intended to boost adoption of similar technologies (Kondylis et al., 2017; Beaman et al., 2021; Ward et al., 2021).

# 1 Background

## 1.1 Conservation Agriculture

Conservation agriculture – characterized by minimal tillage, constant soil cover, and crop rotation – is the world's most widely employed sustainable agriculture production technique, employed on about 12.5% of global cropland as of 2016 (Pretty et al., 2018; Kassam et al., 2019). Conservation agriculture has been promoted as a strategy to both improve agricultural productivity and increase sustainability (Hobbs, 2007). Minimal tillage and soil cover, often achieved through the retention of crop residues, help to increase the biological and moisture content of soil and prevent erosion, while crop rotation is often used as a pest management strategy in the absence of tillage. The techniques at the foundation of conservation agriculture were initially developed to mitigate the soil degradation experienced by dust bowl farmers in the United States (Friedrich et al., 2017). However, it was not until the 1970s that adoption of conservation agriculture practices began in earnest in the United States and around the world.

The rapid adoption of conservation agriculture in the 1970s led to a rush of scientific evaluation. The primary purported benefits of conservation agriculture, reduction of soil erosion, allowance for agricultural production on a wider variety of terrains, reduction of energy and water input needs, and reduction of surface water contamination, have all been found to be valid in experiments and case studies (Phillips et al., 1980). Other potential benefits that have been identified include increased yields, reduced labor requirements, and carbon sequestration. However, the effectiveness of conservation agriculture in providing these particular benefits has been contested (See e.g. Powlson et al. 2014). In particular, the yield benefits of conservation agriculture have been found to vary substantially among agro-ecological conditions and to be near zero on average (Pittelkow et al., 2015). However, most of the available evidence on the benefits of conservation agriculture to date comes from experimental work at research stations or observational work lacking credible causal inference.

### 1.2 CIMMYT and MasAgro

We study a portfolio of extension services provided throughout Mexico that receive methodological and technical backing from CIMMYT through its integrated development programs. In 2007, CIMMYT began to form a plan for 12 regional hubs of agri-food system innovation (Camacho-Villa et al., 2016). These hubs are designed to allow for iterative development of sustainable agriculture techniques and technologies tailored to a specific region. Researchers experimentally evaluate potential techniques in controlled and farmer-participatory experiments. The most successful of these techniques are conveyed through a network of extension technicians to farmers whose feedback and performance data are collected by the technicians to guide further research (Hellin and Camacho, 2017).

In 2010, the Mexican government's *Secretaría de Agricultura, Ganadería, Desarrollo Rural, Pesca y Alimentaría* (SAGARPA)[2] and CIMMYT entered into a partnership with the goal of improving agricultural productivity in Mexico and developing resilience to predicted effects of climate change. SAGARPA substantially increased the funding allocated to the agri-food innovation project, now named MasAgro, in 2012 leading to a subsequent acceleration in its development.

The elements of a CIMMYT hub are divided into four categories: research platforms, modules, extension areas, and impact areas. Research platforms experimentally evaluate production techniques and technologies in order to identify profitable prescriptions for farmers facing a given environment. These experimental plots are typically operated by academic institutions or other agricultural research organizations. Modules are typically set up as side-by-side plots on which a farmer working with an extension technician employs the best practices identified by the research platform network on one plot and conventional practices on the other. Modules allow farmers' knowledge to be integrated with scientific findings from the research platforms to further evaluate agricultural innovation in their context. Extension areas are plots on which a farmer works with a technician to implement some of the practices as developed and fine-tuned in local modules. Impact areas are plots that are known to have adopted techniques or technologies that are locally promoted on modules or extension areas.

[2] The name of SAGARPA was changed in 2018 to *Secretaría de Agricultura y Desarrollo Rural* (SADER).

In order to promote the diffusion of knowledge from research platforms to farmers, as well as to facilitate the incorporation of feedback from farmers into the studies performed at the research platforms, CIMMYT forms partnerships with many private and public extension providers. In addition, CIMMYT hires a relatively small number of technicians who also provide training to other affiliated technicians. While many locations we consider treated in this study previously had agricultural extension in some form, CIMMYT-integration provides technicians with training and knowledge previously unavailable to them. In particular, the sustainable agriculture practices honed at research platforms tend to be relatively new to technicians and farmers. Furthermore, there is evidence that the components of conservation agriculture produce significantly greater yields when used in conjunction than when adopted individually (Pittelkow et al., 2015). Given their novelty, it seems unlikely that these practices would diffuse to these locations in the absence of CIMMYT integration.

Due to the logistic difficulties of establishing a hub, such as securing additional funding and forming partnerships with local research and extension organizations, their development has been staggered. Hubs that were developed earlier operate in regions where CIMMYT was relatively active and already had strong partnerships. As such, the timing of adoption of conservation agriculture techniques is determined, to some extent, by CIMMYT's operations prior to the beginning of MasAgro. However, there is substantial variation in adoption timing within hubs. For example, a number of modules or extension areas may be set up prior to the formal establishment of a hub to facilitate partnership formation and new partnerships with extension providers may induce diffusion in areas within a hub that saw no prior adoption. This is the variation we leverage, along with other exogenous variation such as changes in wind direction, to causally identify the effects of conservation agriculture adoption.

# 2 Data

## 2.1 Extension Service Data

All CIMMYT-affiliated extension services record data in CIMMYT's administrative extension database, the *Bitácora Electrónica MasAgro* (BEM). Data from modules and extension areas are recorded about twice each season while plots are receiving extension services and include details regarding plot characteristics, inputs used, output produced, prices faced, and technologies adopted, along with latitude and longitude of the centroid of the plot. Technicians who learn of other plots on which the technologies they promote are being applied record the data from the plot as an impact area once, including some very basic data on technologies adopted and the plot's centroid. Importantly, the BEM contains the year in which a technician records the impact area, rather than the year of adoption, meaning impact areas may have adopted technologies prior to their appearance in the data. Similarly, technicians do not record data in locations in which they are no longer operating, meaning that the diffusion process may continue without measurement in the BEM.

The BEM contains data on 242,655 plots recorded between 2012 and 2019. Of these, 10,638 are modules, 47,789 are extension areas, and 184,228 are impact areas. The share of plots in each category adopting each of the major promoted technologies is given in table A.2. Notably, conservation agriculture is the most widely adopted technology, employed by nearly a third of all plots recorded in the BEM. Other popular technologies include improved output storage and improved varieties, both adopted by more than a quarter of all impact areas.

## 2.2 Landsat Satellite Imagery Measures

To get a better sense of conservation agriculture adoption beyond what is recorded in the BEM we turn to satellite imagery. In particular the yearly minimum normalized difference tillage index (NDTI) has be very strongly positively correlated with crop residue cover, a practice indicative of conservation agriculture adoption (Zheng et al., 2012). NDTI is calculated as

$$NDTI = \frac{SWIR1 - SWIR2}{SWIR1 + SWIR2}$$

where $SWIR1$ and $SWIR2$ correspond to a shorter and longer wavelength shortwave infrared band[3].

For every year 2001-2020 we process all available Landsat 5, 7, and 8 imagery covering Mexico to mask clouds and apply relevant radiance calibrations. We restrict attention to pixels on agricultural land using the Uso del Suelo IV dataset produced by INEGI, Mexico's national statistical agency. We then calculate NDTI in the unmasked portion of each image and take the pixel-level minimum. Finally, we average these pixel values within each grid cell to obtain our measure of NDTI.

We also measure agricultural productivity using yearly maximum normalized difference vegetation index (NDVI). NDVI is a satellite imagery-derived measure that is strongly correlated with agricultural productivity and has been used as a proxy in previous economics research. NDVI is defined as

$$NDVI = \frac{NIR - Red}{NIR + Red}$$

where $NIR$ refers to the near infrared band and $Red$ refers to the red band. We calculate yearly maximum NDVI using an analogous procedure to that used to calculate NDTI.

### 2.3 Locality Sample and Outcomes

To assess impacts of conservation agriculture diffusion on infant mortality outcomes we use a sample of localities, which are small populated areas roughly analogous to census block groups in the United States. We form our sample of localities from those that existed in the 2000 census. We focus on urban localities because the most populous localities have small agricultural employment shares, suggesting direct effects of extension on infant deaths will be minimal. According to the 2010 *Encuesta Nacional de Ocupación y Empleo*, less than 3% of the population in localities with a population of at least 15,000 were primarily employed in agriculture. As such, any direct benefits of conservation agriculture adoption for farmers, such as greater profits or more available food, should not influence infant mortality in this sample.

[3]For example, the Landsat 5 Thematic Mapper's sensor captures shortwave infrared at 1.55-1.75$\mu$m (SWIR1) and 2.08-2.35$\mu$m (SWIR2).

For the first step of our sample construction we find the set of urban localities that had a population of at least 15,000 in 2010. Because localities tend to split over time, we find the set of localities from the 2000 census that contain the first set. Our final sample, shown in figure 1, consists of the 492 localities that existed in 2000, contain an urban locality that had a population of at least 15,000 in 2010, and have available death data.

Figure 1: Locality Sample

*Notes:* Map of localities included in sample. Borders defined according to 2000 Census.

### Air Quality

To analyze effects of conservation agriculture diffusion on air quality outcomes, we combine two data sets[4]. First, we utilize air quality data from National Air Quality Information System (SINAICA)

[4]We considered using the ground-level $PM_{2.5}$ estimates developed by van Donkelaar et al. (2021), which combine AOD measurements from multiple sensors with a model of chemical transport which is calibrated to approximate ground-based sensor measurements, as an outcome. However, if the predictions suffer from Berkson error, which is

monitor stations. SINAICA stations tend to be located in larger cities; only 74 of the localities in our sample contain a station. These monitors provide measurements of $PM_{10}$, along with a number of other pollutants and weather variables. Measurements are taken hourly, though missing values are fairly common and stations come in and out of service over the course of the study period. We form an unbalanced locality×month-level panel of $PM_{10}$ by first filtering values greater than 600 $\mu g/m^3$ based on the recommendation from SINAICA, then aggregating first to the station×day by taking the maximum, then to station×month and locality×month by taking means.

Second, we calculate monthly mean aerosol optical depth (AOD) as measured by the Moderate Resolution Imaging Spectroradiometer (MODIS) aboard NASA's Terra and Aqua satellites. MODIS data are available daily beginning in February 2000. AOD is a measure of the amount of light diffused between the top of the atmosphere and the surface of the Earth, and has been used in previous studies as a proxy for particulate matter concentration (Zou, 2021; Gendron-Carrier et al., 2022). The main advantage of AOD over air pollution monitor data is spatial coverage. While on a given day, AOD can only be calculated for a relatively small number of 1km×1km pixels, we find that in practice very few locality×months have no observations at all.

**Infant Deaths**

We calculate the number of infant deaths in each locality using publicly available administrative data on all recorded deaths in Mexico from INEGI. To do so, we map the locality of residence listed in the data to its corresponding locality in 2000. We then take the sum of deaths of individuals who were aged less than one year old at the time of death in each locality-month to construct our panel. We also construct a mortality rate by dividing the number of deaths by the living population under one year old at the beginning of the period. Unfortunately, locality information only appear in the publicly available birth data starting in 2013. As such, we limit analyses using infant mortality rate to 2014 and later.

typical of values fitted from a regression, this would tend to attenuate coefficient estimates (Ratledge et al., 2022). Indeed, we document that Berkson error does appear to be present empirically. The slope of the relationship between predicted and observed $PM_{2.5}$ is significantly less than one and the range of predicted values is only about 13% of that of observed values. As expected, estimates using the van Donkelaar et al. (2021) data as outcomes are generally close to zero. Given these results, we focus on observed $PM_{10}$ and AOD.

## 2.4 Wind Data

We determine the daily wind direction in each grid-cell using the ERA5 Reanalysis, which combines data from on-the-ground weather stations with a general climate model to produce daily estimates of a number of weather variables at a $0.25° \times 0.25°$ resolution (Hersbach et al., 2020). Wind data from ERA5 are represented as u- and v-components at 10m height, which correspond to west-to-east and south-to-north components of the wind direction vector.

## 2.5 Agricultural Burning Data

To construct measures of agricultural burning within cells, we use satellite imagery from MODIS. In particular, we utilize the Thermal Anomalies and Fire Version 6 Daily product (MOD14A1), which classifies 1 km $\times$ 1 km pixels as containing active fires or not based on measured radiance in the 4-, 11-, and 12-$\mu$m channels of MODIS imagery while masking non-land pixels (Giglio et al., 2016). While in principle the cause of a given fire cannot be determined in the MODIS active fire data, we label fires "agricultural" if they occur over land marked as used in agriculture, pasture, or forestry in the Uso del Suelo IV dataset.

We aggregate these data to the grid-cell$\times$month-level by summing the number of active fire pixels contained within the cell. As such, this measure specifically records the number of agricultural fire pixels, and may underestimate the number of agricultural fires if there are multiple at the same time within a single 1 km$\times$1 km pixel[5]. For brevity, we refer to this measure as "agricultural fires." In robustness checks we also sum the confidence score assigned by the fire detection algorithm to down-weight relatively uncertain fires.

Figure 2 shows the monthly total number of agricultural fires for grid cells containing at least one plot ever observed in the BEM in each of the years before the introduction of MasAgro. There is strong seasonality in agricultural burning. In general, burning occurs November through June, the period between when maize is generally harvested and planted, with a prominent peak in May. As may be expected, burning plummets during the core of the growing season (July through October).

[5]This measure may also overestimate the number of fires if a single fire spans multiple pixels, although it is very rare to find contiguous fire pixels on the same day in the data.

Figure 2: Cell-Level Burning Seasonality

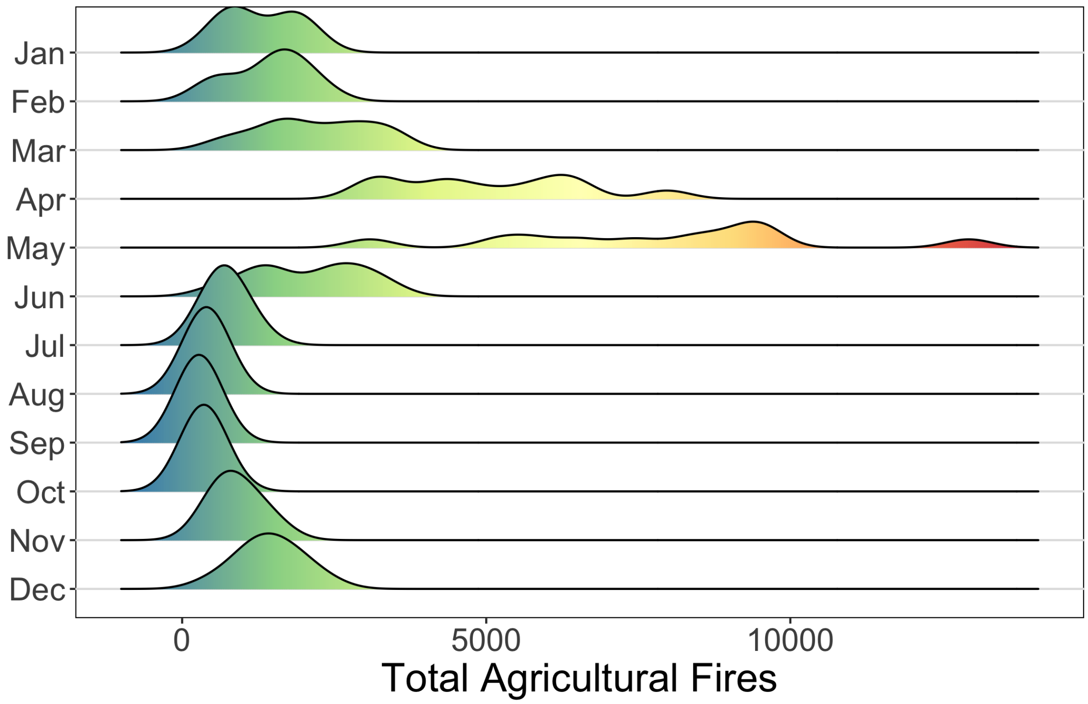


*Notes:* This figure displays distribution of annual agricultural fires between 2002 and 2011 by month.

However, there is heterogeneity in the timing of burning over space, as shown by figure A.1. Fires are also fairly concentrated geographically, as evidenced by figure 3. Most cells average less than one agricultural fire per year, but a small number experience dozens or even hundreds of fires in an average year.

## 3 Diffusion of Conservation Agriculture

We build the diffusion measures used in this study on a grid of $0.1° \times 0.1°$ cells[6] covering the extent of Mexico. This size was chosen to capture the spatial heterogeneity in the roll-out of extension services while yielding a manageable number of cells.

We consider two measures of the extent of conservation agriculture diffusion. The first and more

[6] $0.1°$ is approximately 11 Km.

Figure 3: Cell-Level Burning Prevalence

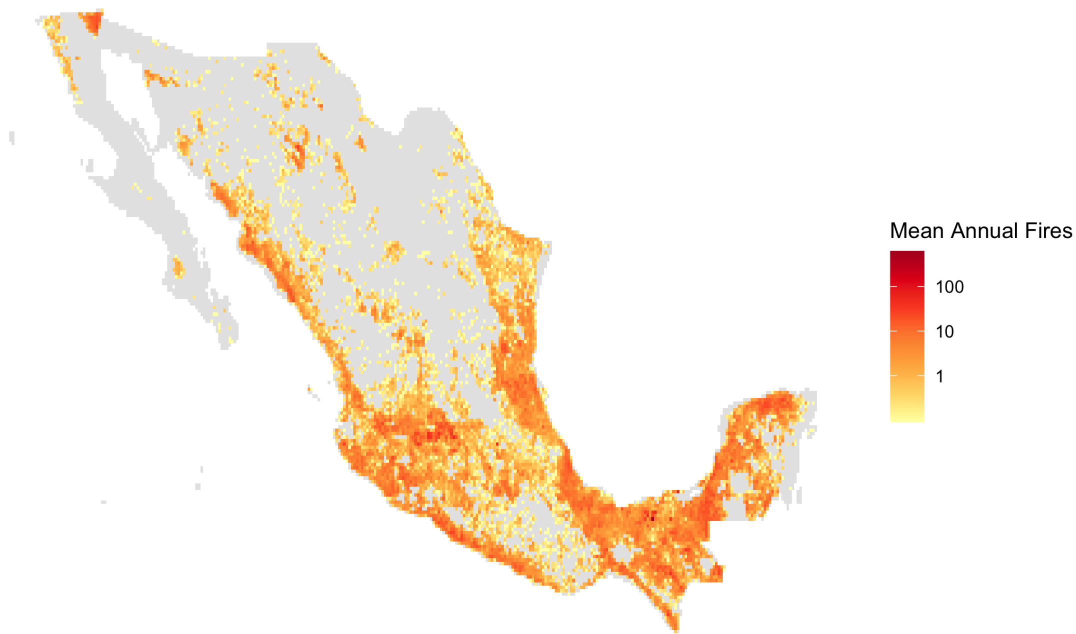


*Notes:* Each $0.1° \times 0.1°$ is colored according to its mean number of agricultural fire pixels. Means are constructed using data from 2001-2011. Grey pixels have no agricultural fires between 2001 and 2011.

coarse measure is whether or not a cell contains any plot that has appeared in the BEM and is recorded as adopting conservation agriculture. To facilitate brevity later on, we introduce notation to define our measures. Let $f(i)$ denote the first year that plot $i$ appears in the BEM as having adopted conservation agriculture[7]. We define $BEM_{ct} = 1\{\sum_{i \in c} 1\{t \geq f(i)\} > 0\}$, an indicator for cell $c$ containing at least one plot in the BEM that has adopted conservation agriculture by year $t$. It will also be useful to keep track of the set of cells that see any conservation agriculture adoption. To this end, we define $Ever_{ct} = 1\{\sum_{t=2012}^{2019} BEM_{ct} > 0\}$, an indicator for the cell containing a plot that ever appears in the BEM as having adopted conservation agriculture.

Figure 4 shows the resulting grid of year assignments. Note that there is substantial heterogene-

[7]Only the year and agricultural cycle (spring-summer or autumn-winter) is recorded. As such, we simply assign treatment at the year level, rather than a finer temporal scale.

ity in treatment timing even over small areas. This variation will be combined with wind direction to identify the causal effect of conservation agriculture adoption on locality level outcomes. It will also serve as the basis for an event study exploring the effects of conservation agriculture adoption on our mechanism of interest, agricultural burning.

The second diffusion measure incorporates information on the area of plots. Let $area(i)$ be the area of plot $i$. We define $BEM\ Area_{ct} = \sum_{i \in c} 1\{t \geq f(i)\} \times area(i)$, the area of plots in the BEM that have adopted conservation agriculture.

Figure 4: Cell Treatment Timing

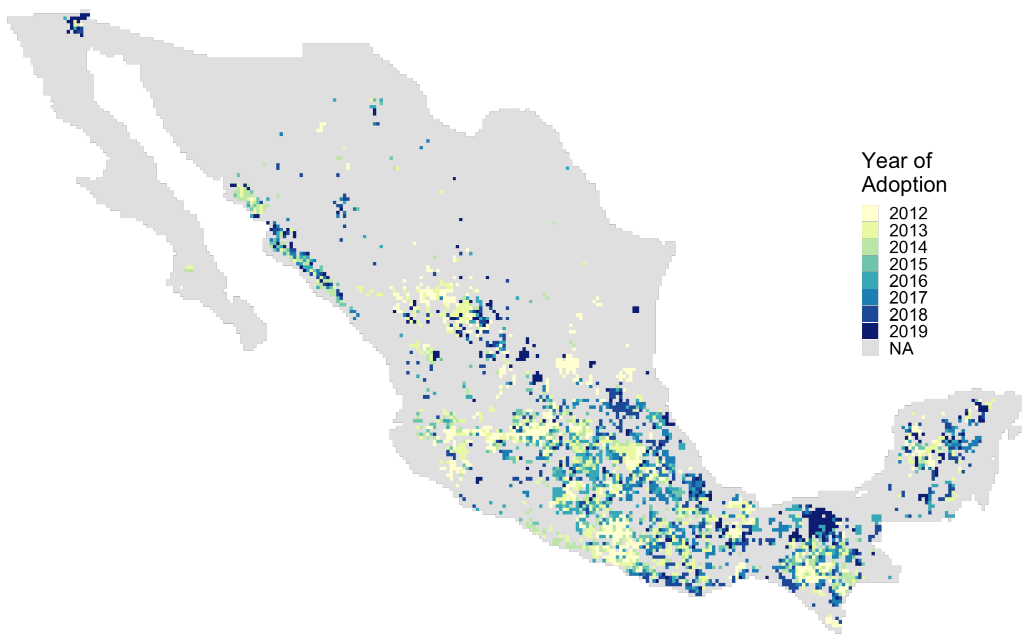


*Notes:* $0.1^\circ \times 0.1^\circ$ grid cells colored by the first year a plot within their extent received CIMMYT-affiliated extension services. Gray cells did not receive extension between 2012 and 2019.

To measure diffusion at the locality level, we assign grid cells within 50km of a locality's centroid to that locality. In particular, for a locality $l$, we define $N(l)$ to be the set of grid cells within 50km of $l$'s centroid and construct the variables $Near\ BEM_{lt} = \sum_{c \in N(l)} BEM_{ct}$ and $Near\ BEM\ Area_{lt} = \sum_{c \in N(l)} BEM\ Area_{ct}$. Note that any given cell can be assigned to multiple localities.

Because data recorded in the BEM is limited to locations where extension technicians are currently operating it may not capture the full extent of conservation agriculture diffusion. The diffusion process may continue after technicians leave an area or end their affiliation with CIMMYT. Similarly, conservation agriculture may diffuse to a location prior to the arrival of extension and only be recorded later. To get a sense of how our diffusion measures correspond to the level of conservation agriculture adoption we turn to our panel of NDTI observations.

To estimate the effects of conservation agriculture adoption on NDTI we employ an event study design. Due to noted issues with two-way fixed effect (TWFE) estimators (Goodman-Bacon, 2021; Sun and Abraham, 2021), we implement the imputation estimation procedure outlined by Borusyak et al. (2021). We posit a model of the untreated potential outcome for cell $i$ located in state $s(i)$ in year $t$

$$NDTI(0)_{it} = \alpha_i + \delta_{s(i)t} + \Gamma' X_{it} + \varepsilon_{it} \tag{1}$$

which is estimated using observed outcomes for cells that have not yet received extension, or never do. $X_{it}$ is a vector of controls, namely total precipitation and average temperature for each month of the year. We then predict untreated potential outcomes and estimate observation-specific treatment effects for cells that have received extension as $\widehat{\tau_{it}} = NDTI(1)_{it} - \widehat{NDTI(0)}_{it}$. Dynamic treatment effects are estimated as

$$\beta^k = \frac{1}{|\{it : t - f(i) = k\}|} \sum_{it:t-f(i)=k} \widehat{\tau_{it}} \tag{2}$$

where $f(i)$ denotes the first year that plot $i$ appears in the BEM as having adopted conservation agriculture. As shown by Borusyak et al. (2021), this estimator is consistent even under staggered treatment roll-out and unrestricted treatment effect heterogeneity, which is not the case for the TWFE estimator.

To analyze pre-trends, we augment equation (1) with pre-treatment event time indicators, omitting the 10 years pre-treatment indicator as it is the first pre-treatment indicator shared by all

Figure 5: Effect of MasAgro on Conservation Tillage

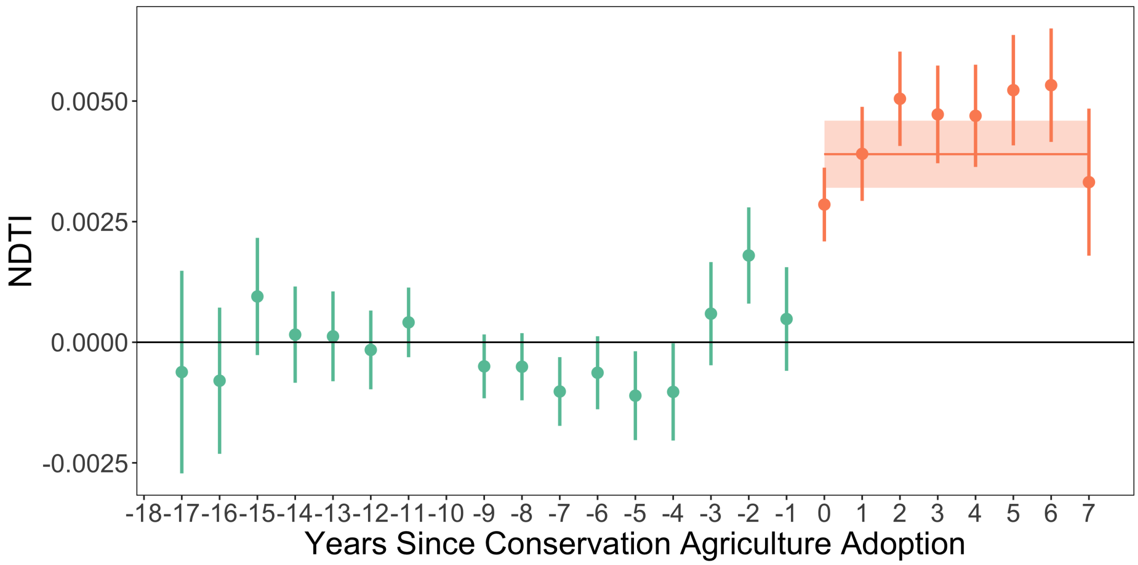


*Notes:* This figure shows the effect of conservation agriculture adoption on NDTI. The sample is composed of 8,300 grid cells with at least 5% agricultural land coverage observed for each year 2002-2019 to produce a dataset of 149,400 observations. The are 119 observations with missing NDTI measurement due limited imagery availability. The x-axis denotes the number of years since conservation agriculture adoption in the grid cell, with negative values indicating years prior to adoption. Pre-trends, shown in green, are estimated using the specification given by equation (3) and 95% confidence intervals are constructed from standard errors clustered at the grid cell level. Post-treatment estimates, shown in orange, are calculated according to equation (2) and 95% confidence intervals are constructed from conservative estimates of standard errors clustered at the grid cell level following Borusyak et al. (2021). The orange bar in the post-period is the difference-in-differences estimate and its 95% confidence interval is given by the orange shaded rectangle.

ever-treated cells. The pre-trend specification is given by

$$NDTI(0)_{it} = \alpha_i + \delta_{s(i)t} + \sum_{k \in \Omega^{pre}} \beta_k 1\{t - f(i) = k\} + \Gamma' X_{it} + \varepsilon_{imt} \tag{3}$$

where $\Omega^{pre} = \{-18, -17, ..., -11, -9, -8, ..., -1\}$.

Figure 5 displays the event study estimation results. Reassuringly, most pretrend coefficient estimates are relatively small in magnitude and statistically insignificant. There is a statistically significant increase two years before the arrival of MasAgro, though the following year sees a subsequent decrease and the effect is no longer statistically significant. In the year of conservation adoption as measured by the BEM there is a large and statistically significant increase in NDTI of

0.0029, or about 2% of the mean. Subsequent years see further increases, leveling off three years after conservation agriculture adoption. Based on the linear relationship estimated by Zheng et al. (2012), the difference-in-difference estimate suggests that crop residue cover increases by 2.8% after conservation agriculture adoption is recorded in the BEM.

These results demonstrate that conservation agriculture adoption as recorded by the BEM corresponds to a discrete increase in NDTI, a proxy for crop residue cover and conservation tillage that is observable in satellite imagery. The diffusion process appears to continue up to three years after the arrival of MasAgro extension. The lack of notable pre-trends lends credibility to the interpretation that conservation agriculture adoption causes the increase in NDTI.

# 4 Economic Impacts of Conservation Agriculture Adoption

## 4.1 Profits

We first explore farmer profits by analyzing the BEM data for modules. Recall that modules consist of a business-as-usual plot and a plot operated by the same farmer that employs technologies suggested by an extension technician. While it is unlikely that there is no selection into which modules employ conservation agriculture, we suspect there is minimal selection into which plot employs the MasAgro technologies, although it was not explicitly randomized.

We assess the profitability of plots employing conservation agriculture and other promoted technologies to the business-as-usual plots by comparing the empirical cumulative density functions for profits per hectare, plotted in figure 6. Extension plots have greater profits at almost every point in the distribution and a Kolmogorov-Smirnov test supports the hypothesis that extension plots first order stochastically dominate conventional plots at the 1% level for plots that employ conservation agriculture. The first order stochastic dominance test statistic is not significant for non-conservation agriculture technologies, but this appears to be driven by the tails of the distribution. As such, all MasAgro technologies seem to be substantial improvements over the status quo in terms of farmers' profits.

We also perform a simple test of the relative profitability of extension plots that do and do not

Figure 6: Profit Distribution by Technology

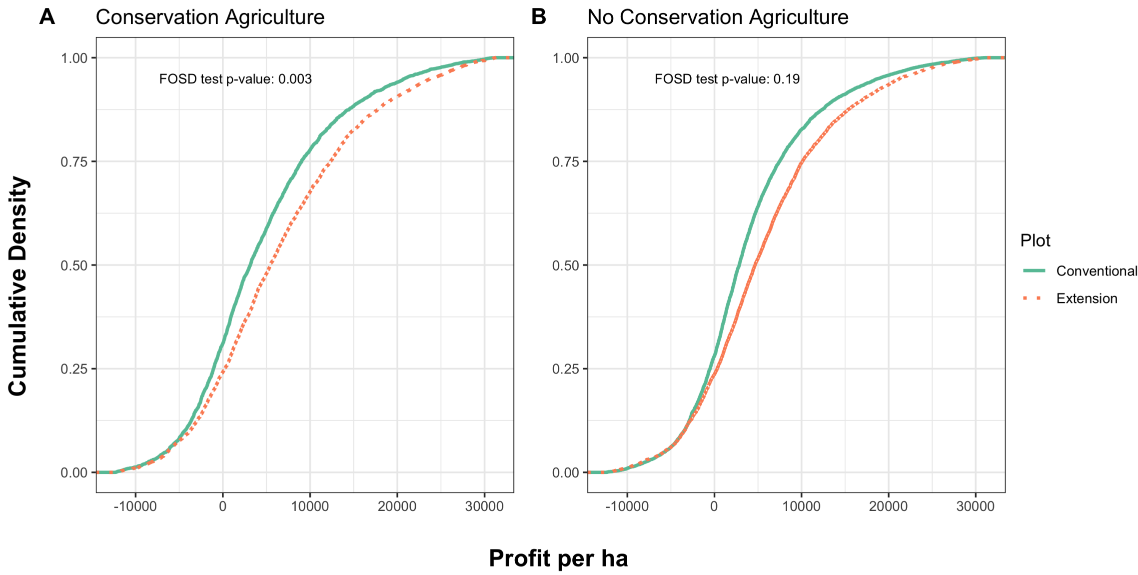


*Notes:* Plot-level empirical cumulative density functions of profit per hectare by treatment status and technologies adopted. P-values reported are for a Kolmogorov-Smirnov test of the null hypothesis that the Extension distribution does not first order stochastically dominate the Conventional distribution.

employ conservation agriculture with the following regression.

$$profit_{pft} = \alpha_{ft} + \beta^E Extension_p + \beta^{CA} Extension_p \times CA_f + \varepsilon_{pt} \tag{4}$$

In equation (4), $p$ indexes plots, $f$ indexes modules (or equivalently, producers), $t$ indexes years, $Extension$ is an indicator for the plot employing MasAgro-promoted technologies, and $CA$ is an indicator for conservation agriculture being employed on the module's extension plot. We Winsorize the top and bottom 2.5% of profit observations because of the presence of implausibly large magnitudes.

Estimates of equation (4) are shown in Table 1. Our estimate of $\beta^E$ is 1,738 pesos per hectare, or 0.41 in logs, and is statistically significant at the 1% level, reinforcing the finding above that extension plots are more profitable. Our estimate of $\beta^{CA}$ is 585 pesos, and is also significant at the 1% level, implying that farmers who employ conservation agriculture earn *more* than farmers who

Table 1: Effects Conservation Agriculture on Profits

| Outcome | Profit/ha | log(Profit/ha) |
|---|---|---|
| | (1) | (2) |
| Extension | 1737.7 | 0.407 |
| | (58.8) | (0.012) |
| | [<0.01] | [<0.01] |
| Extension × CA Module | 584.8 | 0.020 |
| | (111.3) | (0.022) |
| | [<0.01] | [0.36] |
| Observations | 24098 | 17700 |

*Notes:* Profits are top and bottom Winsorized at 2.5%. All regressions include field fixed effects. Standard errors clustered at the producer-level are in parentheses. P-values are in brackets.

do not. The magnitude of the effect is also substantial, our estimates suggest that conservation agriculture plots earn about 33% greater profits than plots employing other technologies promoted by extension. However, when we use log profit per hectare as the outcome we estimate a very small and statistically insignificant $\beta^{CA}$. This difference in results may be due to the sample restriction to plots with positive profits. Together, these results suggest that MasAgro technologies substantially increase the profits earned by farmers, and that at worst conservation agriculture does not appear to lower profitability.

## 4.2 Agricultural Productivity

While the profit analysis above suggests that conservation agriculture is profitable in the short run, it cannot speak to longer term effects on agricultural productivity. To that end we turn to our NDVI dataset, which allows us to observe a continuous time series of proxy for agricultural productivity.

We implement the same imputation event study estimator as was used in the previous section to study the effects of conservation agriculture adoption on NDVI. The results of this estimation procedure are shown in figure 7. Pre-trend estimates are generally close to 0 and statistically insignificant. There does appear to be a slight anticipation effect in the year prior to conservation

Figure 7: Event Study of the Effects of Conservation Agriculture on Agricultural Productivity

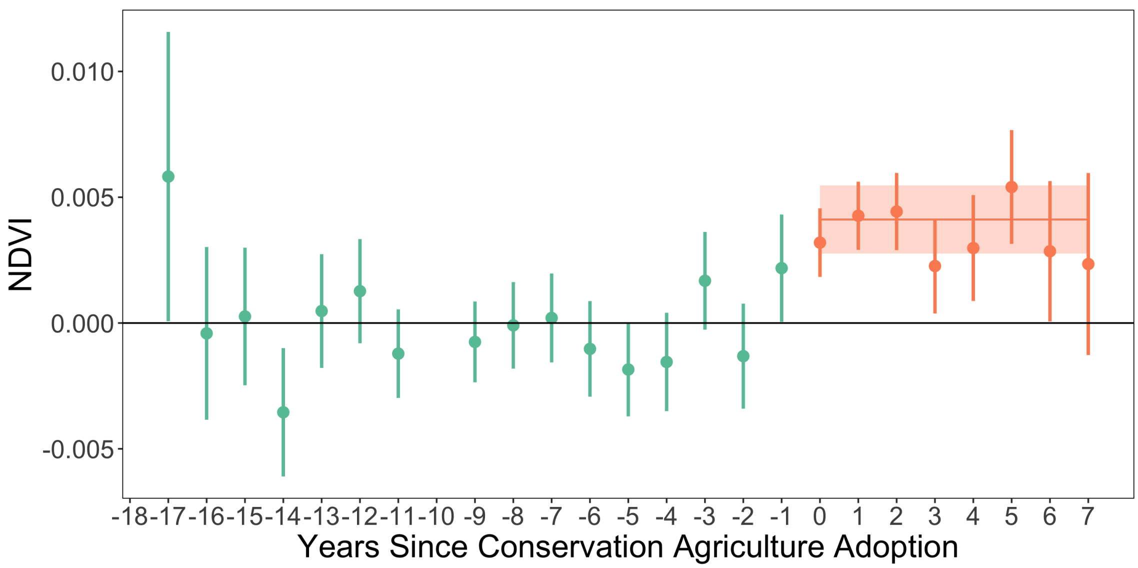


*Notes:* This figure shows the effect of conservation agriculture adoption on NDVI. The sample is composed of 8,300 grid cells with at least 5% agricultural land use observed for each year 2002-2019 to produce a dataset of 149,400 observations. The are 119 observations with missing NDVI measurement due limited imagery availability. The x-axis denotes the number of years since conservation agriculture adoption in the grid cell, with negative values indicating years prior to adoption. Pre-trends, shown in green, are estimated using the specification given by equation (3) and 95% confidence intervals are constructed from standard errors clustered at the grid cell level. Post-treatment estimates, shown in orange, are calculated according to equation (2) and 95% confidence intervals are constructed from conservative estimates of standard errors clustered at the grid cell level following Borusyak et al. (2021). The orange bar in the post-period is the difference-in-differences estimate and its 95% confidence interval is given by the orange shaded rectangle.

agriculture adoption. This may occur because some cells adopt other promoted technologies prior to adopting conservation agriculture.

There is a notable increase in NDVI after conservation agriculture adoption however. All post-adoption estimates are positive and range from 0.002-0.006, or 0.3-0.9% of the pre-2012 mean NDVI. Estimates for the year of adoption and six following years are all statistically significant at the 5% level. While the estimates for the seventh year after adoption is not statistically significant this may be due to limited statistical power given the relatively small sample the estimate is identified from. The difference-in-difference estimate suggests that NDVI increases by about 0.6% of the pre-2012 mean after the adoption of conservation agriculture.

The results on NDVI suggest that conservation agriculture adoption leads to an increase in agricultural productivity. Furthermore, this increase is persistent, with estimates out to five years post-adoption of similar magnitude and statistically significant. The large economic benefits of conservation agriculture adoption suggest that a market friction, most likely imperfect information, inhibits adoption prior to the arrival of extension.

# 5 Effects of Conservation Agriculture Diffusion on Urban Air Pollution and Infant Mortality

Our identification strategy relies on exogenous changes in exposure to conservation agriculture due to wind variation. For a given locality, we consider the set of cells within 50 km. The locality is designated "downwind" from a grid cell on a given day if the locality's centroid is within the 45° cone with vertex at the cell's centroid pointing in the direction of the wind vector in the cell[8]. Figure 8 shows this visually, with the smaller locality in the bottom-left being "downwind" from the white cell. This measure is based on the direction of the wind in the location of emission, rather than the location of outcome measurement as is typical, which may reduce measurement error. The indicator for "downwind" is interacted with $BEM_{ct}$ and the sum is taken over cell×days associated

[8]More explicitly, if $\theta$ represents the angle between the vector pointing from the cell's centroid to the locality's centroid and the vector pointing from the cell's centroid in the wind direction then a locality is downwind if $cos(\theta) \geq cos(\pi/8)$.

Figure 8: Illustration of "Downwind" Definition

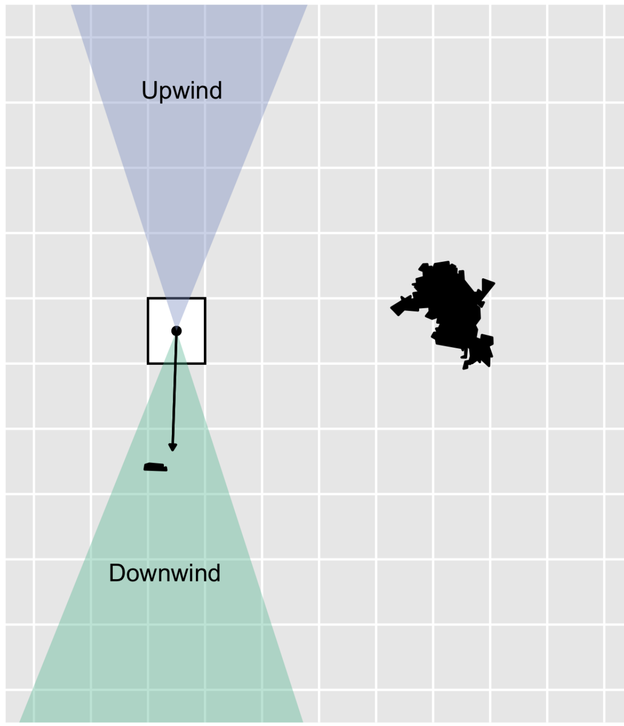


*Notes:* This figure illustrates how localities, shown in black, are determined to be downwind from a cell. The white grid lines correspond to cell boundaries. The arrow points in the direction of the prevailing wind direction in the white cell. The green cone extending in the direction of the wind vector is "downwind," while the purple cone extending in the opposite direction is "upwind." The small locality just below the white cell is "downwind", while the large locality to the right is "lateral" to the white cell.

with the locality×month. Finally, we normalize this sum by the total number of days to make a measure of downwind locality-months.

Concretely, let $Downwind_{cldmt}$ indicate that locality $l$ is downwind of cell $c$ on day $d$ of month $m$ of year $t$. The measure described above is defined as

$$Downwind\ BEM_{lmt} = \frac{1}{|\{d \in m\}|} \sum_{c \in N(l)} \sum_{d \in m} Downwind_{cldmt} \times Near\ BEM_{ct}$$

A value of 1 for this measure means that on an average day in the month the locality's centroid was downwind from one grid-cell within 50km containing at least one plot that has adopted conservation agriculture. Similar measures are constructed for the locality being upwind from cells and being neither upwind nor downwind (which we refer to as "lateral"), as well as using the area-based diffusion measure and the indicator for a cell containing a plot that ever adopts conservation agriculture.

Our first specification is inspired by the one utilized by Rangel and Vogl (2019) to measure the effects of agricultural burning on birth outcomes. We compare the effect of a locality being downwind from cells which contain a plot that has adopted conservation agriculture before and after adoption. In particular, we estimate

$$Y_{ltm} = \alpha_{lm} + \delta_t + \beta Downwind\ BEM_{ltm} + \gamma_1 Near\ BEM_{lt} + \gamma_2 Downwind\ Ever_{ltm} + \varepsilon_{ltm} \quad (5)$$

where $Y$ is a measure of air quality or infant mortality rate and $Downwind\ BEM$ is defined above. Locality×month ($\alpha_{lm}$) and year ($\delta_t$) fixed effects are included to isolate plausibly exogenous variation due to wind realizations. When the number of infant deaths is used as an outcome we estimate an analogous Poisson regression with an exponential link function given that the outcome is a count variable with many zeros and a long right tail and improvements in air quality likely cause reductions in the number of infant deaths proportional to population.

Controlling for the number of cells within 50km that have adopted conservation agriculture, $Near\ BEM_{lt}$, is important because localities with greater conservation agriculture adoption nearby may be on different trends than localities with less nearby adoption. Put in the language of design-based inference, we need to condition on the number of cells that have adopted conservation agriculture to isolate exogenous variation in the number of those cells the locality is downwind from.

Including the number of cells within 50km that ever adopt conservation agriculture that the locality is downwind from, $Downwind\ Ever_{ltm}$, allows cells that adopt conservation agriculture to differentially affect the outcome. Omitting this control may induce omitted variable bias if, for example, cells that adopt conservation agriculture have higher baseline levels of agricultural burning, which is empirically true. Heuristically, the specification in equation (5) compares the effect of being downwind from a cell that adopts conservation agriculture before adoption to after adoption.

To explore seasonality in these effects, we estimate a similar specification in which the effects of cells are allowed to vary by month of year

$$\begin{aligned} Y_{ltm} = \alpha_{lm} + \delta_t + \sum_{n=1}^{12} 1\{m = n\} \times [ \\ \beta_n^{down} Downwind\ BEM_{ltm} + \\ \gamma_n^{up} Downwind\ Ever_{ltm}] + \\ \gamma^{near} Near\ BEM_{it} + \varepsilon_{ltm}. \end{aligned} \tag{6}$$

Because the independent variable of interest is measured on a 50km radius around localities' centroids, it is especially important to account for spatial autocorrelation when conducting statistical inference. To this end, we default to using heteroskedasticity and autocorrelation robust standard errors with a 100km uniform spatial kernel (Conley, 1999). This will tend to produce more conservative standard error estimates than clustering at the locality level.

Table 2 presents the estimated coefficients of equation (5). Notably, *Downwind BEM* has a negative effect on both $PM_{10}$ and the number of infant deaths. A locality spending one month downwind from one additional cell containing a plot that has adopted conservation agriculture is estimated to reduce $PM_{10}$ concentration by 1.3%, aerosol optical depth by 0.895, or about 4.96% of the mean. The difference in relative magnitudes of these estimates may be because SINAICA monitors are mostly located in larger cities, where a smaller share of air pollution may be attributable to distant agricultural sources.

Air quality improvements generated by conservation agriculture diffusion appear to translate into sizeable reductions in infant mortality. A one unit increase in *Downwind BEM* reduces the number of infant deaths by 1.29% and the infant mortality rate by 21.3 deaths per 10,000 living. These effects are large, though not out of line with past research. Arceo et al. (2016) estimate that a 1 $\mu$g/m$^3$ increase in weekly $PM_{10}$ concentration increases infant mortality by 2.31 deaths per

100,000 living in Mexico City. We estimate that a one unit increase in *Downwind BEM* causes a 1.3% decrease in monthly mean $PM_{10}$ concentration, which corresponds to about 1.5 $\mu g/m^3$. Given the estimates of Arceo et al. (2016), this would imply an increase of about 13.9 infant deaths per 100,000 living, about two-thirds of the effect we estimate. However, we cannot reject the null hypothesis that our estimates are the same[9].

We also run a placebo version of equation (5) using *Upwind BEM* in place of *Downwind BEM* and *Upwind Ever* in place of *Downwind Ever*. Reassuringly, the resulting coefficient estimates for *Upwind BEM* are comparatively small in magnitude (except in the case of $PM_{10}$), of the opposite sign, and not statistically significant at conventional levels. This suggests that the wind variation is capturing meaningful variation in the transport of air pollution. The placebo test also suggests that our results are not due solely to localities with greater conservation adoption potentially being selected on more rapidly improving air quality. Rather, the differences in estimates depending on the wind direction analyzed are indicative of greater exposure to conservation agriculture causing improvements in air quality and, subsequently, infant health.

Panel B of Table 2 presents estimates using *BEM Area* as the diffusion measure. Results are qualitatively similar, though less precisely estimated. Notably, the estimated effects on $PM_{10}$ and infant mortality rate are no longer statistically significant. When using *Upwind BEM Area* as the diffusion measure the estimated coefficients are again generally insignificant. This may be due to the limited capacity of technicians to observe and record all adoption, especially after outreach ceases in an area. Given that the total area cultivated under conservation agriculture is likely noisily measured, it is perhaps unsurprising that precision suffers.

We next explore the seasonality of the effects of *Downwind BEM* on $PM_{10}$ concentration and infant deaths. Panel A of Figure 9 shows that there are relatively large reductions in $PM_{10}$ concentration during the months of March through June, and October. All of those months' estimated coefficients are on the order of a 2% reduction and statistically significant at the 5% level, except May, which is significant at the 10% level. This pattern of effects generally corresponds to

[9] We also estimate an analogous IV and obtain a point estimate of -454.75 which is statistically significant at the 10% level, though the first stage F-statistic is quite low at 2.05. Again, we cannot reject that this is different from the estimate of Arceo et al. (2016), though these results should be interpreted with caution given the lack of statistical precision.

Table 2: Effects of Conservation Agriculture Diffusion on Infant Deaths by Wind Direction

| Outcome | $\log(PM_{10})$ | AOD | Infant Deaths (%) | Infant Mortality Rate |
|---|---|---|---|---|
| | (1) | (2) | (3) | (4) |
| *Panel A: BEM* | | | | |
| Downwind | -0.013 | -0.895 | -1.286 | -21.352 |
| | (0.006) | (0.307) | (0.311) | (8.911) |
| | [0.02] | [<0.01] | [<0.01] | [0.02] |
| Upwind | 0.023 | 0.429 | 0.264 | 5.326 |
| | (0.018) | (0.319) | (0.749) | (6.978) |
| | [0.20] | [0.18] | [0.72] | [0.45] |
| *Panel B: BEM Area* | | | | |
| Downwind | -0.002 | -0.424 | -0.921 | -1.472 |
| | (0.008) | (0.121) | (0.233) | (2.230) |
| | [0.76] | [<0.01] | [<0.01] | [0.51] |
| Upwind | 0.029 | 0.138 | -0.047 | -0.999 |
| | (0.022) | (0.086) | (0.423) | (2.624) |
| | [0.20] | [0.11] | [0.91] | [0.70] |
| Mean Outcome | 4.623 | 257.741 | 277.874 | 198.416 |
| Observations | 8929 | 87675 | 106200 | 21495 |

*Note:* Each coefficient and standard error estimate corresponds to a separate estimation of a variant of equation (5). $PM_{10}$ is available for localities with SINAICA stations and is an unbalanced panel. AOD is also an unbalanced panel, with missing observations for locality-months where no cloud-fee images are available. Coefficients in the Infant Deaths column are estimated via Poisson regression. Infant Mortality Rate is in deaths per 10,000 living and is only available from 2013 onward. Conley (1999) standard errors with a uniform spatial kernel of 100km in parentheses.

what we would expect given that conservation agriculture is likely to reduce air pollution during periods of land management. June is at the end of planting period for the spring-summer maize cycle and October is at the beginning of the harvest period.

Infant mortality does not display the same seasonality. Rather, reductions in infant mortality are consistently experienced throughout the year. Other than the estimated coefficient for May, which is significant at the 10% level, all effects are significant at the 1% level and range from about 1-2.5% reductions in the number of infant deaths. The largest reductions are seen in December through February. This pattern of results may be due to temporal autocorrelation in *Downwind BEM* leading to the estimated coefficients incorporating the effects of improvements in air quality in previous months. For example, the estimate for December may be especially large in magnitude thanks to the reductions in $PM_{10}$ in October. Results using hectares of plots that have adopted conservation agriculture as the diffusion measure are qualitatively similar, but less precise (see Figure A.4).

We test this hypothesis of autocorrelation using a collection of specifications which include temporal lags of *Downwind BEM*. These results are shown in Appendix Table A.5. We find that across all specifications, effects are concentrated on the month before observing the infant mortality outcome. There is also some evidence of an effect from the fifth month prior to observation, though this effect is not statistically significant when we include 12 month lags. To summarize, our results suggest that conservation agriculture adoption led to declines in infant mortality in nearby localities via reduced air pollution. Our most preferred estimate suggests that absent conservation agriculture, the average locality in the sample would have experienced 7.06% more infant deaths in 2019. As previous studies have found adverse health consequences in the general population associated with air pollution in general (Schlenker and Walker, 2016) and with agricultural burning in particular (He et al., 2020), the true benefits of conservation agriculture are likely much greater than we have considered.

Figure 9: Seasonality of the Effects of Conservation Agriculture Diffusion

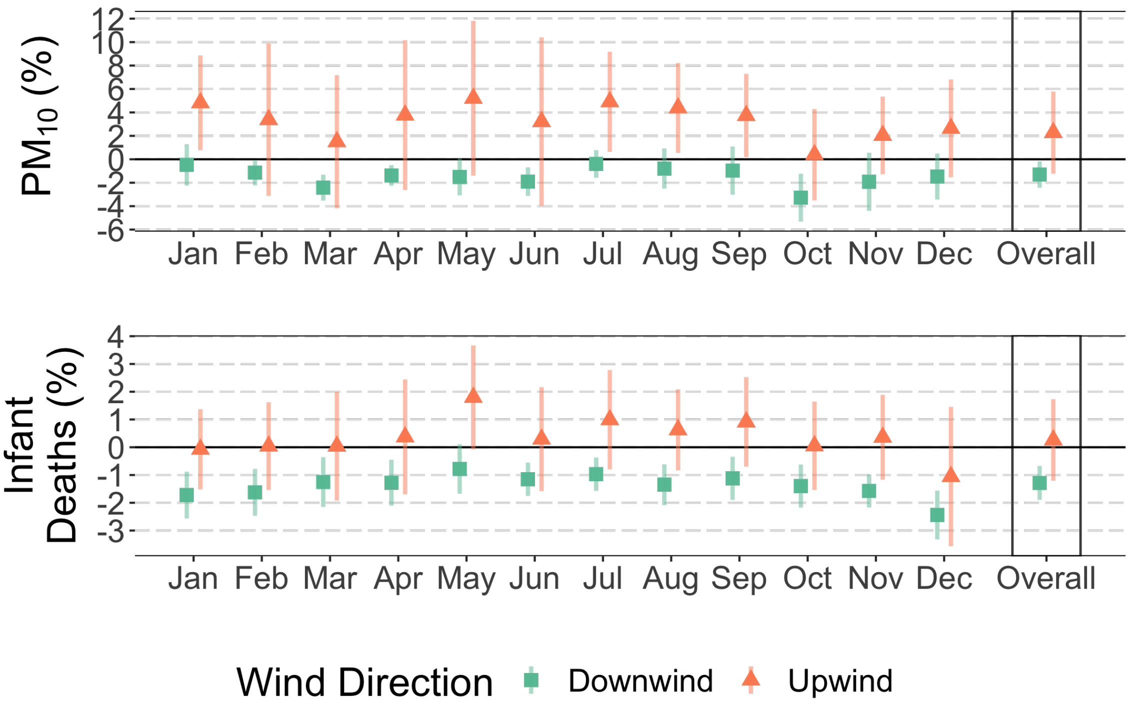


*Notes:* Coefficient estimates from equation (6) (all point estimates and confidence intervals are from one regression except for "Overall," which comes from equation (5)). Confidence intervals are calculated from Conley (1999) heteroskedasticity and autocorrelation robust standard errors with a uniform spatial kernel of 100 Km radius. Table A.4 displays point estimates and standard errors.

## 5.1 Monthly Deaths Averted and Program Costs

To compare estimated benefits to the costs of implementation, we only consider benefits due to reduced infant mortality. Note that there are many other potential benefits due to reduced air pollution produced by crop residue burning, as well as the benefits to farmers suggested by our profit analysis above, that we omit. Because our estimates cannot tell us how much longer babies live compared to the counterfactual with no extension, calculating an estimate of the number of infant deaths averted requires additional assumptions.

We opt for a set of simple back-of-the-envelope calculations. In the first, we assume that each averted death is unique and that all infants whose deaths were averted live to adulthood. While admittedly an optimistic set of assumptions, this will allow us to approximate the benefits of reduced infant mortality based on our estimate in table 2. Using the value of statistical life in Mexico calculated by de Lima (2020) in 2011 USD of $211,406, this method values the 11,959.09 estimated deaths averted at $2,528,222,421, over 33 times the program's cost. Alternatively, we calculate the share of the number of implied infant deaths averted that would have to be converted into adult lives saved for the program to "break even" and find that only 3% of these deaths recover the entire cost of the program.

# 6 Mechanism: Agricultural Burning

In this section, we describe the research designs we use to estimate the effects of conservation agriculture diffusion on agricultural burning and present results of the estimation. In this section we focus on the presence of plots in the BEM that are recorded as employing conservation agriculture as our adoption measure of interest.

## 6.1 Event Study and Difference-in-Differences

To estimate the effects of the diffusion of MasAgro-promoted technologies on agricultural burning, we again employ the imputation event study estimator.

Results for equations 2-3 are shown in figure 10. While there appears to be a slight reduction in agricultural burning in the year before any plot appears in the BEM, no pre-event coefficient estimates are significant at the 5% level. This may be due to the nature of adoption measurement in impact areas, which constitute the majority of observations in the BEM and are necessarily observed with some delay in adoption. All post-adoption estimates are negative and fairly close to -0.5, but only the coefficient for the year of adoption is statistically significant. The exception is the final event time coefficient, which is notably larger in magnitude but still statistically insignificant. The difference-in-differences estimate suggests that monthly agricultural fires declined by 0.5 and is significant at the 10% level.

Because of the strong seasonality of agricultural burning, we are also interested in evaluating the

Figure 10: Year-Level Agricultural Fire Event Study

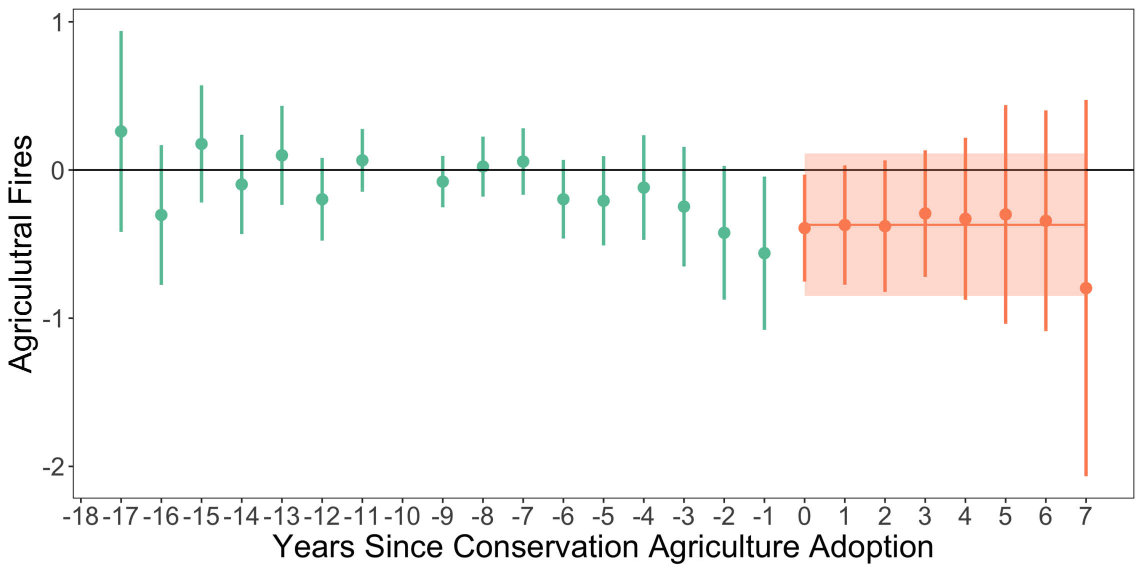


*Notes:* 95% confidence intervals for pre-treatment event time coefficients are constructed from standard errors clustered at the cell. 95% confidence intervals for post-treatment event time coefficients are constructed from conservative standard error estimates clustered at the cell level following Borusyak et al. (2021). The horizontal line across the post period is the difference-in-differences estimate and the shaded box is its 95% confidence interval constructed from conservative standard error estimates clustered at the cell level following Borusyak et al. (2021). The sample includes all cells that have at least 20% of their area dedicated to agricultural land and adopt conservation agriculture or do not contain a plot which appears in the BEM.

effects in particular months. To do so, we re-estimate the imputation event study at the cell-month level, rather than cell-year level, and average observation-specific treatment effect estimates within months.

$$\beta^{DiD_n} = \frac{1}{|\{imt : t - f(i) \geq 0 \& m = n\}|} \sum_{imt:t-f(i)\geq 0 \& m=n} \widehat{\tau_{imt}}. \tag{7}$$

We also estimate a spatial fixed effects (SFE) specification (Goldstein and Udry, 2008; Conley and Udry, 2010; Magruder, 2012). This specification allows for very fine differential trends in burning by comparing a grid cell to those immediately surrounding it. Concretely, let $N(i)$ denote the set of cells in the $7 \times 7$ grid of cells centered on cell $i$[10]. We estimate the specification

$$\begin{aligned}
[Ag.\ Fires_{imt} - \frac{1}{|\{j : j \in N(i)\}|} \sum_{j \in N(i)} Ag.\ Fires_{jmt}] = [\alpha_{im} - \gamma_{N(i)m}] + \\
\sum_{n=1}^{12} \beta_{SFE}^{DiD_n} [BEM_{imt} - \frac{1}{|\{j : j \in N(i)\}|} \sum_{j \in N(i)} BEM_{jmt}] \times 1\{m = n\} + \\
[\varepsilon_{imt} - \frac{1}{|\{j : j \in N(i)\}|} \sum_{j \in N(i)} \varepsilon_{jmt}] \qquad (8)
\end{aligned}$$

which accounts for local time trends by subtracting off the mean outcome in a cell's immediate vicinity. Intuitively, as long as the unobserved time trends are similar in cell $i$ and $N(i)$, differencing within time periods removes these effects.

While this method can control for local time trends it does suffer from issues that are less salient in the BJS estimation procedure. First, the negative weighting issues associated with TWFE also arise with SFE when already-treated cells serve as "controls" for cells becoming treated. Second, spatial spillovers loom large in this setting, as cells are only compared to their immediate neighbors. We suspect that the most likely source of spillovers is unobserved technology diffusion, which would tend to bias our results towards zero. Third, differencing off the outcomes of nearby cells mechanically introduces spatial dependence in the error terms. To deal with this last issue, we utilize the standard error estimator introduced by Conley (1999), allowing errors to be correlated up to a 100km radius.

The month-specific difference-in-difference estimates of equation 7 are shown in panel A of Figure 11. Reductions in burning appear to be especially concentrated in June and November, which all experience declines of greater than 1 agricultural fire after the introduction of promoted technologies. July and December also see marginally significant reductions in the number of agricultural fires. All other months experience non-significant changes. Notably, this pattern of results aligns well with the reductions in downwind locality $PM_{2.5}$ concentration shown in Figure 9.

The estimates of the SFE specification are shown in panel B of Figure 11. The results are

[10]In practice, some neighborhoods are do not contain all 49 cells because they lie close to the edge of the country's boundary.

Figure 11: Effects of Conservation Agriculture on Agricultural Fires by Month

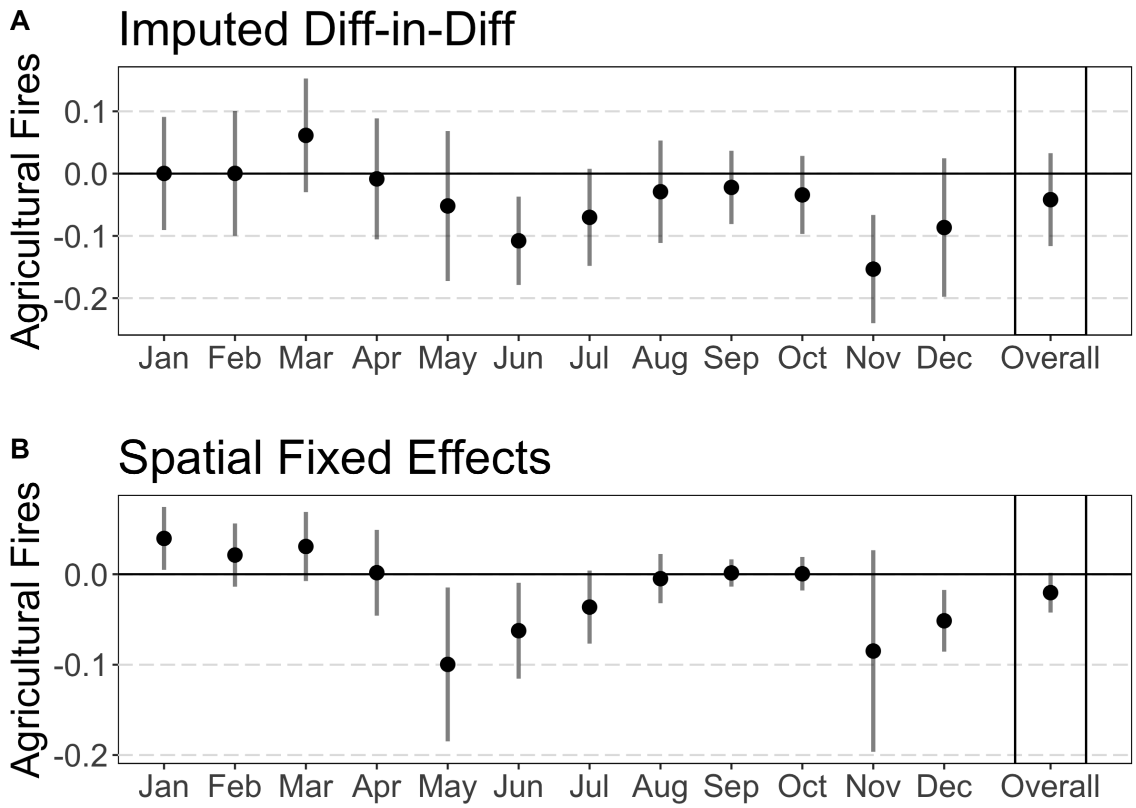


*Notes:* Coefficient estimates and 95% confidence intervals from equation 7 are shown in Panel A. Standard errors in Panel A are conservative estimates clustered at the cell level following Borusyak et al. (2021). The sample in Panel A includes all cells that have a median number of agricultural fires per year greater than zero prior to 2012. Coefficient estimates and 95% confidence intervals from equation 8 are shown in Panel B. Confidence intervals in Panel B are constructed using heteroskedasticity and autocorrelation robust standard error estimates with a 100km uniform spatial kernel following Conley (1999). The sample in Panel B is all cells have strictly positive agricultural land area according to the Soil Use Map Version IV.

qualitatively and quantitatively similar to the results in Panel A, with statistically significant declines observed in May, June, and December and a marginally significant decline in July. Again, these results suggest that reductions in crop residue burning may be partially responsible for the downwind improvements in air quality and infant health observed in the main results.

As a robustness check, we estimate the same specifications using fires that occur off of agricultural land as the outcome. Given that conservation agriculture adoption should only affect burning through the use of crop residues, we would not expect meaningful results off of agricultural land. Figure A.6 shows that the post adoption level of non-agricultural burning is not statistically different at conventional levels. We also do not estimate meaningful reductions in non-agricultural burning in any month, but do find slight increases in March (Figure A.7).

# 7 Conclusion

In this paper, we evaluated the economic and environmental impacts of the diffusion of conservation agriculture, the world's most widely practiced sustainable intensification technique. Using data collected by extension technicians on the location and timing of conservation agriculture adoption, we first showed that adoption causes a statistically significant increase in NDTI, a satellite observed proxy for conservation tillage and crop residue cover. Using prior estimates from the remote sensing literature suggests that crop residue cover in a $0.1^\circ \times 01^\circ$ grid cell increases by 2.8% after a plot within the cell adopts conservation agriculture.

Contrary to popular belief, we find that conservation agriculture adoption is immediately profitable when we compare side-by-side extension-advised and business-as-usual plots. This may be due to the more tailored suggestions afforded by receiving extension assistance along with the adoption of additional, complimentary technologies such as improved varieties. Notably, conservation agriculture also appears to be weakly more profitable that other technology packages promoted by MasAgro. We also find evidence of an increase in agricultural productivity as measured by satellite imagery after conservation agriculture adoption using a totally distinct research design. These results suggest the existence of substantial information frictions which limit the adoption and diffusion of conservation agriculture in the absence of extension.

In addition to the positive economic effects of conservation agriculture adoption there are very large environmental benefits. Using variation in the amount of land employing conservation agriculture a locality is downwind from, we find that the diffusion of conservation agriculture translates to large reductions in particulate matter concentration and infant deaths. In terms of mechanisms, we find large decreases in agricultural burning during planting and harvest months, consistent with the timing of air quality improvements in downwind localities.

Viewed as a policy to reduce infant mortality, we find the extension programs studied have been cost effective. Our preferred estimates imply that CIMMYT-backed extension led to a reduction of 11,421.48 infant deaths over the 2012-2019 period. Multiplying this reduction by the value of statistical life in Mexico suggests that the benefits of the program in terms of reduced infant mortality are an order of magnitude greater than its cost of implementation. The fact that the promoted technologies were not intended to abate air pollution in urban areas coupled with the geographic and temporal concentration of agricultural burning suggests that a well-targeted policy may prove even more cost effective.

Conservation agriculture extension appears to be a rare win-win environmental policy in the Mexican context. This study suggests that there may be large environmental benefits to sustainable intensification, in this case many times greater than the costs of promoting adoption.

## References

E. Arceo, R. Hanna, and P. Oliva. Does the Effect of Pollution on Infant Mortality Differ Between Developing and Developed Countries? Evidence from Mexico City. *The Economic Journal*, 126(591):257–280, Mar. 2016. ISSN 00130133. doi: 10.1111/ecoj.12273. URL `https://academic.oup.com/ej/article/126/591/257-280/5077419`.

L. Beaman, A. BenYishay, J. Magruder, and A. M. Mobarak. Can Network Theory-Based Targeting Increase Technology Adoption? *American Economic Review*, 111 (6):1918–1943, June 2021. ISSN 0002-8282. doi: 10.1257/aer.20200295. URL `https://pubs.aeaweb.org/doi/10.1257/aer.20200295`.

A. P. Behrer and D. Lobell. Higher levels of no-till agriculture associated with lower PM 2.5 in the Corn Belt. *Environmental Research Letters*, 17(9): 094012, Sept. 2022. ISSN 1748-9326. doi: 10.1088/1748-9326/ac816f. URL `https://iopscience.iop.org/article/10.1088/1748-9326/ac816f`.

K. Borusyak, X. Jaravel, and J. Spiess. Revisiting Event Study Designs: Robust and Efficient Estimation. 2021. doi: 10.48550/ARXIV.2108.12419. URL `https://arxiv.org/abs/2108.12419`. Publisher: arXiv Version Number: 3.

T. C. Camacho-Villa, C. Almekinders, J. Hellin, T. E. Martinez-Cruz, R. Rendon-Medel, F. Guevara-Hernández, T. D. Beuchelt, and B. Govaerts. The evolution of the MasAgro hubs: responsiveness and serendipity as drivers of agricultural innovation in a dynamic and heterogeneous context. *The Journal of Agricultural Education and Extension*, 22(5):455–470, Oct. 2016. ISSN 1389-224X, 1750-8622. doi: 10.1080/1389224X.2016.1227091. URL `https://www.tandfonline.com/doi/full/10.1080/1389224X.2016.1227091`.

K. G. Cassman and P. Grassini. A global perspective on sustainable intensification research. *Nature Sustainability*, 3(4):262–268, Apr. 2020. ISSN 2398-9629. doi: 10.1038/s41893-020-0507-8. URL `https://www.nature.com/articles/s41893-020-0507-8`.

T. Conley. GMM estimation with cross sectional dependence. *Journal of Econometrics*, 92(1):1–45, Sept. 1999. ISSN 03044076. doi: 10.1016/S0304-4076(98)00084-0. URL `https://linkinghub.elsevier.com/retrieve/pii/S0304407698000840`.

T. G. Conley and C. R. Udry. Learning about a New Technology: Pineapple in Ghana. *American Economic Review*, 100(1):35–69, Mar. 2010. ISSN 0002-8282. doi: 10.1257/aer.100.1.35. URL `https://pubs.aeaweb.org/doi/10.1257/aer.100.1.35`.

M. de Lima. The value of a statistical life in Mexico. *Journal of Environmental Economics and Policy*, 9(2):140–166, Apr. 2020. ISSN 2160-6544, 2160-6552. doi: 10.1080/21606544.2019.1617196. URL `https://www.tandfonline.com/doi/full/10.1080/21606544.2019.1617196`.

J. M. Deines, S. Wang, and D. B. Lobell. Satellites reveal a small positive yield effect from conservation tillage across the US Corn Belt. *Environmental Research Letters*, 14(12):124038, Dec. 2019. ISSN 1748-9326. doi: 10.1088/1748-9326/ab503b. URL `https://iopscience.iop.org/article/10.1088/1748-9326/ab503b`.

O. Erenstein. Crop residue mulching in tropical and semi-tropical countries: An evaluation of residue availability and other technological implications. *Soil and Tillage Research*, 67(2):115–133, Sept. 2002. ISSN 01671987. doi: 10.1016/S0167-1987(02)00062-4. URL `https://linkinghub.elsevier.com/retrieve/pii/S0167198702000624`.

T. Friedrich, R. Derpsch, and A. Kassam. Chapter 3 Overview of the Global Spread of Conservation Agriculture. In K. Etingoff, editor, *Sustainable Development of Organic Agriculture*, pages 53–68. Apple Academic Press, 3333 Mistwell Crescent, Oakville, ON L6L 0A2, Canada, Jan. 2017. ISBN 978-1-77188-483-9 978-1-77188-484-6. doi: 10.1201/9781315365800-4. URL `http://www.crcnetbase.com/doi/10.1201/9781315365800-4`.

N. Gendron-Carrier, M. Gonzalez-Navarro, S. Polloni, and M. A. Turner. Subways and Urban Air Pollution. *American Economic Journal: Applied Economics*, 14(1): 164–196, Jan. 2022. ISSN 1945-7782, 1945-7790. doi: 10.1257/app.20180168. URL `https://pubs.aeaweb.org/doi/10.1257/app.20180168`.

L. Giglio, W. Schroeder, and C. O. Justice. The collection 6 MODIS active fire detection algorithm and fire products. *Remote Sensing of Environment*, 178:31–41, June 2016. ISSN 00344257. doi: 10.1016/j.rse.2016.02.054. URL `https://linkinghub.elsevier.com/retrieve/pii/S0034425716300827`.

H. C. J. Godfray. The debate over sustainable intensification. *Food Security*, 7(2):199–208, Apr. 2015. ISSN 1876-4517, 1876-4525. doi: 10.1007/s12571-015-0424-2. URL `http://link.springer.com/10.1007/s12571-015-0424-2`.

H. C. J. Godfray, J. R. Beddington, I. R. Crute, L. Haddad, D. Lawrence, J. F. Muir, J. Pretty, S. Robinson, S. M. Thomas, and C. Toulmin. Food Security: The Challenge of Feeding 9 Billion People. *Science*, 327(5967):812–818, Feb. 2010. ISSN 0036-8075, 1095-9203. doi: 10.1126/science.1185383. URL `https://www.science.org/doi/10.1126/science.1185383`.

M. Goldstein and C. Udry. The Profits of Power: Land Rights and Agricultural Investment in Ghana. *Journal of Political Economy*, 116(6):981–1022, Dec. 2008. ISSN 0022-3808, 1537-534X. doi: 10.1086/595561. URL `https://www.journals.uchicago.edu/doi/10.1086/595561`.

A. Goodman-Bacon. Difference-in-differences with variation in treatment timing. *Journal of Econometrics*, 225(2):254–277, Dec. 2021. ISSN 03044076. doi: 10.1016/j.jeconom.2021.03.014. URL `https://linkinghub.elsevier.com/retrieve/pii/S0304407621001445`.

J. Graff Zivin, T. Liu, Y. Song, Q. Tang, and P. Zhang. The unintended impacts of agricultural fires: Human capital in China. *Journal of Development Economics*, 147:102560, Nov. 2020. ISSN 03043878. doi: 10.1016/j.jdeveco.2020.102560. URL `https://linkinghub.elsevier.com/retrieve/pii/S0304387820301358`.

R. M. Gunton, L. G. Firbank, A. Inman, and D. M. Winter. How scalable is sustainable intensification? *Nature Plants*, 2(5):16065, May 2016. ISSN 2055-0278. doi: 10.1038/nplants.2016.65. URL `http://www.nature.com/articles/nplants201665`.

G. He, T. Liu, and M. Zhou. Straw burning, PM2.5, and death: Evidence from China. *Journal of Development Economics*, 145:102468, June 2020. ISSN 03043878. doi: 10.1016/j.jdeveco.2020.102468. URL `https://linkinghub.elsevier.com/retrieve/pii/S0304387820300432`.

J. Hellin and C. Camacho. Agricultural research organisations' role in the emergence of agricultural innovation systems. *Development in Practice*, 27(1):111–115, Jan. 2017. ISSN 0961-4524, 1364-9213. doi: 10.1080/09614524.2017.1256373. URL https://www.tandfonline.com/doi/full/10.1080/09614524.2017.1256373.

H. Hersbach, B. Bell, P. Berrisford, S. Hirahara, A. Horányi, J. Muñoz-Sabater, J. Nicolas, C. Peubey, R. Radu, D. Schepers, A. Simmons, C. Soci, S. Abdalla, X. Abellan, G. Balsamo, P. Bechtold, G. Biavati, J. Bidlot, M. Bonavita, G. Chiara, P. Dahlgren, D. Dee, M. Diamantakis, R. Dragani, J. Flemming, R. Forbes, M. Fuentes, A. Geer, L. Haimberger, S. Healy, R. J. Hogan, E. Hólm, M. Janisková, S. Keeley, P. Laloyaux, P. Lopez, C. Lupu, G. Radnoti, P. Rosnay, I. Rozum, F. Vamborg, S. Villaume, and J. Thépaut. The ERA5 global reanalysis. *Quarterly Journal of the Royal Meteorological Society*, 146(730):1999–2049, July 2020. ISSN 0035-9009, 1477-870X. doi: 10.1002/qj.3803. URL https://onlinelibrary.wiley.com/doi/10.1002/qj.3803.

P. R. Hobbs. Conservation agriculture: what is it and why is it important for future sustainable food production? *The Journal of Agricultural Science*, 145(02):127, Apr. 2007. ISSN 0021-8596, 1469-5146. doi: 10.1017/S0021859607006892. URL http://www.journals.cambridge.org/abstract_S0021859607006892.

A. Kassam, T. Friedrich, and R. Derpsch. Global spread of Conservation Agriculture. *International Journal of Environmental Studies*, 76(1):29–51, Jan. 2019. ISSN 0020-7233, 1029-0400. doi: 10.1080/00207233.2018.1494927. URL https://www.tandfonline.com/doi/full/10.1080/00207233.2018.1494927.

F. Kondylis, V. Mueller, and J. Zhu. Seeing is believing? Evidence from an extension network experiment. *Journal of Development Economics*, 125:1–20, Mar. 2017. ISSN 03043878. doi: 10.1016/j.jdeveco.2016.10.004. URL https://linkinghub.elsevier.com/retrieve/pii/S0304387816300827.

W. Lai, S. Li, Y. Li, and X. Tian. Air Pollution and Cognitive Functions: Evidence from Straw Burning in China. *American Journal of Agricultural Economics*, 104 (1):190–208, Jan. 2022. ISSN 0002-9092, 1467-8276. doi: 10.1111/ajae.12225. URL https://onlinelibrary.wiley.com/doi/10.1111/ajae.12225.

J. Loos, D. J. Abson, M. J. Chappell, J. Hanspach, F. Mikulcak, M. Tichit, and J. Fischer. Putting meaning back into "sustainable intensification". *Frontiers in Ecology and the Environment*, 12(6):356–361, Aug. 2014. ISSN 1540-9295. doi: 10.1890/130157. URL http://doi.wiley.com/10.1890/130157.

J. R. Magruder. High Unemployment Yet Few Small Firms: The Role of Centralized Bargaining in South Africa. *American Economic Journal: Applied Economics*, 4 (3):138–166, July 2012. ISSN 1945-7782, 1945-7790. doi: 10.1257/app.4.3.138. URL https://pubs.aeaweb.org/doi/10.1257/app.4.3.138.

N. Mahon, I. Crute, E. Simmons, and M. M. Islam. Sustainable intensification – "oxymoron" or "third-way"? A systematic review. *Ecological Indicators*, 74: 73–97, Mar. 2017. ISSN 1470160X. doi: 10.1016/j.ecolind.2016.11.001. URL https://linkinghub.elsevier.com/retrieve/pii/S1470160X16306380.

J. D. Michler, K. Baylis, M. Arends-Kuenning, and K. Mazvimavi. Conservation agriculture and climate resilience. *Journal of Environmental Economics and Management*, 93:148–169, Jan. 2019. ISSN 00950696. doi: 10.1016/j.jeem.2018.11.008. URL `https://linkinghub.elsevier.com/retrieve/pii/S0095069617307532`.

D. J. Pannell, R. S. Llewellyn, and M. Corbeels. The farm-level economics of conservation agriculture for resource-poor farmers. *Agriculture, Ecosystems & Environment*, 187:52–64, Apr. 2014. ISSN 01678809. doi: 10.1016/j.agee.2013.10.014. URL `https://linkinghub.elsevier.com/retrieve/pii/S016788091300354X`.

R. E. Phillips, R. L. Blevins, G. W. Thomas, W. W. Frye, and S. H. Phillips. No-Tillage Agriculture. *Science*, 208(4448):1108–1113, June 1980.

C. M. Pittelkow, X. Liang, B. A. Linquist, K. J. van Groenigen, J. Lee, M. E. Lundy, N. van Gestel, J. Six, R. T. Venterea, and C. van Kessel. Productivity limits and potentials of the principles of conservation agriculture. *Nature*, 517(7534):365–368, Jan. 2015. ISSN 0028-0836, 1476-4687. doi: 10.1038/nature13809. URL `http://www.nature.com/articles/nature13809`.

D. S. Powlson, C. M. Stirling, M. L. Jat, B. G. Gerard, C. A. Palm, P. A. Sanchez, and K. G. Cassman. Limited potential of no-till agriculture for climate change mitigation. *Nature Climate Change*, 4(8):678–683, Aug. 2014. ISSN 1758-678X, 1758-6798. doi: 10.1038/nclimate2292. URL `http://www.nature.com/articles/nclimate2292`.

J. Pretty, T. G. Benton, Z. P. Bharucha, L. V. Dicks, C. B. Flora, H. C. J. Godfray, D. Goulson, S. Hartley, N. Lampkin, C. Morris, G. Pierzynski, P. V. V. Prasad, J. Reganold, J. Rockström, P. Smith, P. Thorne, and S. Wratten. Global assessment of agricultural system redesign for sustainable intensification. *Nature Sustainability*, 1(8):441–446, Aug. 2018. ISSN 2398-9629. doi: 10.1038/s41893-018-0114-0. URL `http://www.nature.com/articles/s41893-018-0114-0`.

H. K. Pullabhotla, M. Zahid, S. Heft-Neal, V. Rathi, and M. Burke. Global biomass fires and infant mortality. *Proceedings of the National Academy of Sciences*, 120(23): e2218210120, June 2023. ISSN 0027-8424, 1091-6490. doi: 10.1073/pnas.2218210120. URL `https://pnas.org/doi/10.1073/pnas.2218210120`.

M. A. Rangel and T. S. Vogl. Agricultural Fires and Health at Birth. *The Review of Economics and Statistics*, 101(4):616–630, Oct. 2019. ISSN 0034-6535, 1530-9142. doi: 10.1162/rest˙a˙00806. URL `https://direct.mit.edu/rest/article/101/4/616/58569/Agricultural-Fires-and-Health-at-Birth`.

N. Ratledge, G. Cadamuro, B. De La Cuesta, M. Stigler, and M. Burke. Using machine learning to assess the livelihood impact of electricity access. *Nature*, 611(7936):491–495, Nov. 2022. ISSN 0028-0836, 1476-4687. doi: 10.1038/s41586-022-05322-8. URL `https://www.nature.com/articles/s41586-022-05322-8`.

W. Schlenker and W. R. Walker. Airports, Air Pollution, and Contemporaneous Health. *The Review of Economic Studies*, 83(2):768–809, Apr. 2016. ISSN 0034-6527, 1467-937X. doi: 10.1093/restud/rdv043. URL `https://academic.oup.com/restud/article-lookup/doi/10.1093/restud/rdv043`.

L. Sun and S. Abraham. Estimating dynamic treatment effects in event studies with heterogeneous treatment effects. *Journal of Econometrics*, 225(2):175–199, Dec. 2021. ISSN 03044076. doi: 10.1016/j.jeconom.2020.09.006. URL `https://linkinghub.elsevier.com/retrieve/pii/S030440762030378X`.

J. A. Tambo and J. Mockshell. Differential Impacts of Conservation Agriculture Technology Options on Household Income in Sub-Saharan Africa. *Ecological Economics*, 151:95–105, Sept. 2018. ISSN 09218009. doi: 10.1016/j.ecolecon.2018.05.005. URL `https://linkinghub.elsevier.com/retrieve/pii/S0921800918300375`.

A. van Donkelaar, M. S. Hammer, L. Bindle, M. Brauer, J. R. Brook, M. J. Garay, N. C. Hsu, O. V. Kalashnikova, R. A. Kahn, C. Lee, R. C. Levy, A. Lyapustin, A. M. Sayer, and R. V. Martin. Monthly Global Estimates of Fine Particulate Matter and Their Uncertainty. *Environmental Science & Technology*, 55(22):15287–15300, Nov. 2021. ISSN 0013-936X, 1520-5851. doi: 10.1021/acs.est.1c05309. URL `https://pubs.acs.org/doi/10.1021/acs.est.1c05309`.

P. S. Ward, L. Mapemba, and A. R. Bell. Smart subsidies for sustainable soils: Evidence from a randomized controlled trial in southern Malawi. *Journal of Environmental Economics and Management*, 110:102556, Oct. 2021. ISSN 00950696. doi: 10.1016/j.jeem.2021.102556. URL `https://linkinghub.elsevier.com/retrieve/pii/S0095069621001108`.

B. Zheng, J. B. Campbell, and K. M. De Beurs. Remote sensing of crop residue cover using multi-temporal Landsat imagery. *Remote Sensing of Environment*, 117: 177–183, Feb. 2012. ISSN 00344257. doi: 10.1016/j.rse.2011.09.016. URL `https://linkinghub.elsevier.com/retrieve/pii/S0034425711003439`.

E. Y. Zou. Unwatched Pollution: The Effect of Intermittent Monitoring on Air Quality. *American Economic Review*, 111(7):2101–2126, July 2021. ISSN 0002-8282. doi: 10.1257/aer.20181346. URL `https://pubs.aeaweb.org/doi/10.1257/aer.20181346`.

Table A.1: Locality Descriptive Statistics

| | Minimum | Median | Mean | Maximum | Standard Deviation | N |
|---|---|---|---|---|---|---|
| *Panel A: Localities* | | | | | | |
| BEM (cells) | 0.00 | 43.00 | 38.01 | 82.00 | 25.01 | 492 |
| BEM Area (ha) | 0.00 | 22.07 | 30.64 | 213.60 | 35.54 | 492 |
| *Panel B: Locality-Months* | | | | | | |
| Infant Deaths | 0.00 | 1.00 | 2.78 | 85.00 | 5.49 | 106272 |
| Infant Mortality Rate (per 10,000) | 6.86 | 106.38 | 198.42 | 30000.00 | 539.29 | 21495 |
| $PM_{10}$ ($\mu g/m^3$) | 0.00 | 104.06 | 115.51 | 533.78 | 56.37 | 8950 |
| AOD | 49.15 | 241.45 | 257.74 | 2418.54 | 111.98 | 87675 |

*Note:* Descriptive statistics for locality sample. The variable "BEM (cells)" is the number of 0.1° grid cells within 50km of the locality's centroid that contain at least one plot recorded in the BEM as adopting conservation agriculture. The variable "BEM Area (ha)" is analogous, but counts the total hectares within 50km rather than cells. There are four locality-months with infant mortality rates greater than 1.

Table A.2: Technology adoption shares by plot type

| Technology | Modules | Extension Areas | Impact Areas |
|---|---|---|---|
| Biofertilizers | 0.38 | 0.25 | 0.17 |
| Conservation Agriculture | 0.33 | 0.28 | 0.32 |
| Improved and Adapted Varieties | 0.39 | 0.34 | 0.26 |
| Improved Storage | 0.23 | 0.18 | 0.30 |
| Infrared-optimized Fertilizer | 0.01 | 0.01 | 0.01 |
| New Crop Rotation | 0.07 | 0.05 | 0.05 |
| Non-fertilizer Soil Improvement | 0.11 | 0.07 | 0.07 |
| Soil Analysis | 0.16 | 0.09 | 0.04 |
| Other | 0.34 | 0.28 | 0.26 |

*Note:* Shares of Modules, Extension Areas, and Impact Areas adopting technologies promoted by CIMMYT-backed extension between 2012 and 2019. Plots that appear in the BEM under multiple types (N=5) are assigned according to the priority order Module, Extension Area, Impact Area. Plots can adopt multiple technologies, hence, columns do not sum to 1.

Table A.3: Grid Cell Characteristics

| Variable | Mean | SD | Minimum | Maximum | N |
|---|---|---|---|---|---|
| Night Lights | 0.55 | 2.65 | 0.05 | 136.39 | 18,374 |
| Elevation (m) | 1,000.8 | 812.01 | −4.39 | 3,910.89 | 18,363 |
| Maize Suitability | 3.48 | 2.71 | −0.01 | 8.58 | 18,346 |
| Wheat Suitability | 1.24 | 1.47 | −0.01 | 5.79 | 18,346 |
| Population | 3.81 | 25.28 | 0 | 971.74 | 18,374 |
| Agricultural Land | 0 | 0 | 0 | 0.01 | 18,374 |
| Ever Treated | 0.29 | 0.46 | 0 | 1 | 18,374 |
| Monthly Agricultural Fires | 0.11 | 0.94 | 0 | 228 | 4,189,272 |

Table A.4: Effects of Conservation Agriculture on
Air Quality and Infant Mortality by Wind Direction

| | $PM_{2.5}$ | | Infant Deaths (%) | |
|---|---|---|---|---|
| Month | Downwind BEM | Upwind BEM | Downwind BEM | Upwind BEM |
| January | -0.129 | 0.547 | -1.722 | -0.072 |
| | (0.133) | (0.367) | (0.414) | (0.652) |
| February | -0.502 | 0.003 | -1.624 | 0.041 |
| | (0.137) | (0.430) | (0.387) | (0.688) |
| March | -0.104 | 1.155 | -1.252 | 0.038 |
| | (0.329) | (1.168) | (0.404) | (0.708) |
| April | 0.142 | 1.298 | -1.278 | 0.373 |
| | (0.315) | (0.839) | (0.417) | (0.778) |
| May | -0.080 | 1.554 | -0.783 | 1.798 |
| | (0.127) | (1.155) | (0.462) | (0.815) |
| June | -0.399 | -0.341 | -1.152 | 0.292 |
| | (0.109) | (0.405) | (0.446) | (0.727) |
| July | 0.015 | 0.751 | -0.970 | 0.992 |
| | (0.099) | (0.315) | (0.423) | (0.668) |
| August | -0.132 | 0.348 | -1.346 | 0.628 |
| | (0.103) | (0.287) | (0.366) | (0.616) |
| September | -0.121 | 0.320 | -1.120 | 0.913 |
| | (0.105) | (0.269) | (0.475) | (0.670) |
| October | -0.598 | -0.291 | -1.398 | 0.052 |
| | (0.131) | (0.265) | (0.468) | (0.613) |
| November | -0.386 | 0.147 | -1.573 | 0.360 |
| | (0.125) | (0.298) | (0.395) | (0.656) |
| December | -0.552 | -0.254 | -2.440 | -1.055 |
| | (0.123) | (0.406) | (0.441) | (0.839) |
| Overall | -0.167 | 0.017 | -1.286 | 0.264 |
| | (0.097) | (0.218) | (0.265) | (0.436) |
| Observations | 4746 | 4746 | 106200 | 106200 |

Table A.5: IV Estimate of $PM_{2.5}$ on Infant Mortality

| | Infant Morality Rate (per 10,000) |
|---|---|
| $PM_{2.5}$ | 0.820 |
| | (0.424) |
| 1st Stage F-Stat | 1.923 |
| p-value | 0.004 |
| Observations | 2856 |

Instruments include Upwind BEM and Upwind Ever interacted with month indicators. Heteroskedasticity and autocorrelation robust standard errors with a 100km uniform spatial kernel constructed following Conley (1999) in parentheses.

Figure A.1: Cell-Level Burning Seasonality

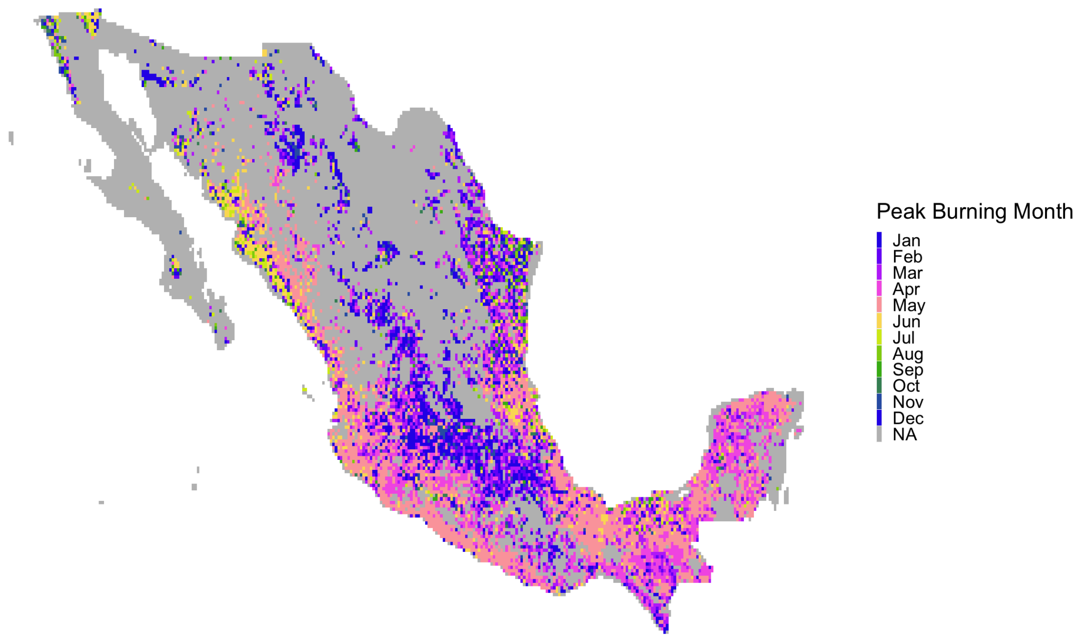


*Notes:* Each $0.1^{\circ} \times 0.1^{\circ}$ is colored according to the month of the year in which agricultural burning tends to peak. Means are constructed using data from 2001-2011.

Figure A.2: Seasonality of the Effects of Conservation Agriculture Diffusion: Upwind

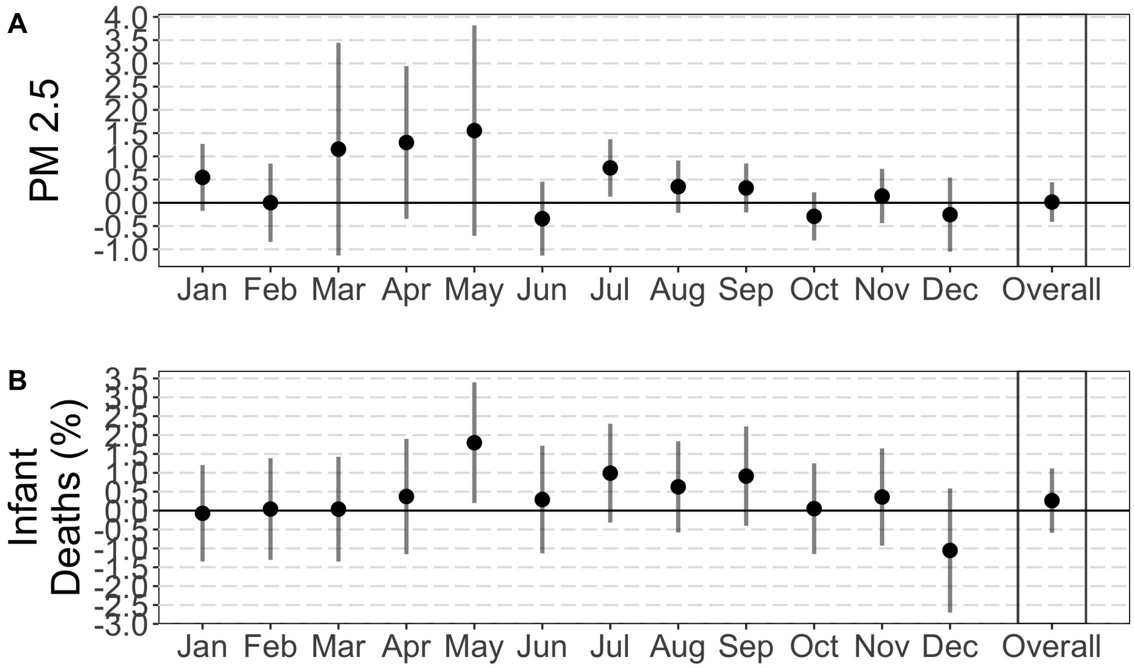


*Notes:* Coefficient estimates from equation (6) (all point estimates and confidence intervals are from one regression except for "Overall," which comes from equation (5)). Confidence intervals are calculated from Conley (1999) heteroskedasticity and autocorrelation robust standard errors with a uniform spatial kernel of 100 Km radius. Table A.4 displays point estimates and standard errors.

Figure A.3: Effects of Conservation Agriculture on AOD and GWR $PM_{2.5}$

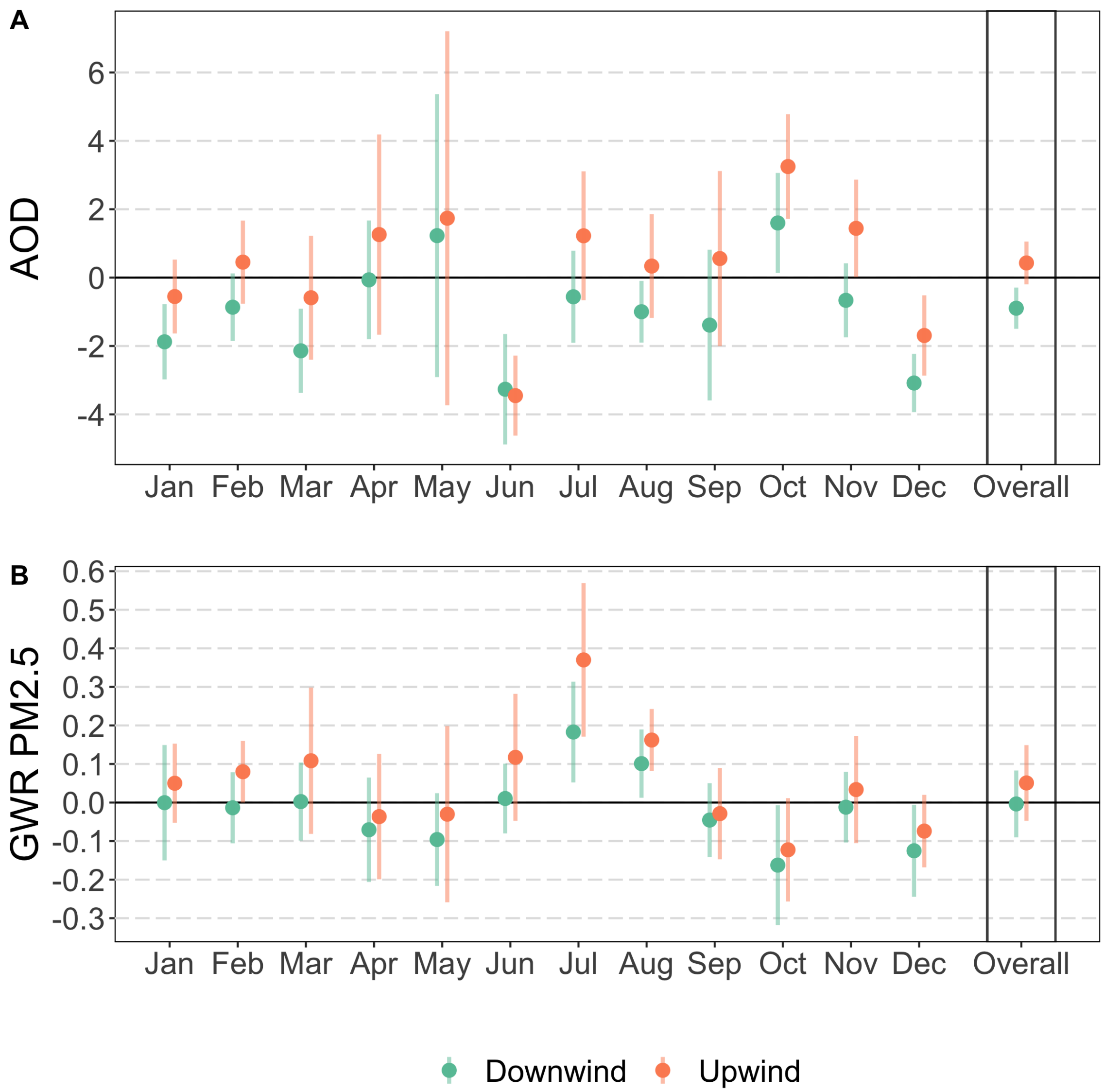


*Notes:* Coefficient estimates from equation (6) (all point estimates and confidence intervals are from one regression except for "Overall," which comes from equation (5)). Confidence intervals are calculated from Conley (1999) heteroskedasticity and autocorrelation robust standard errors with a uniform spatial kernel of 100 Km radius.

Figure A.4: Effects of Conservation Agriculture Adoption by Hectares

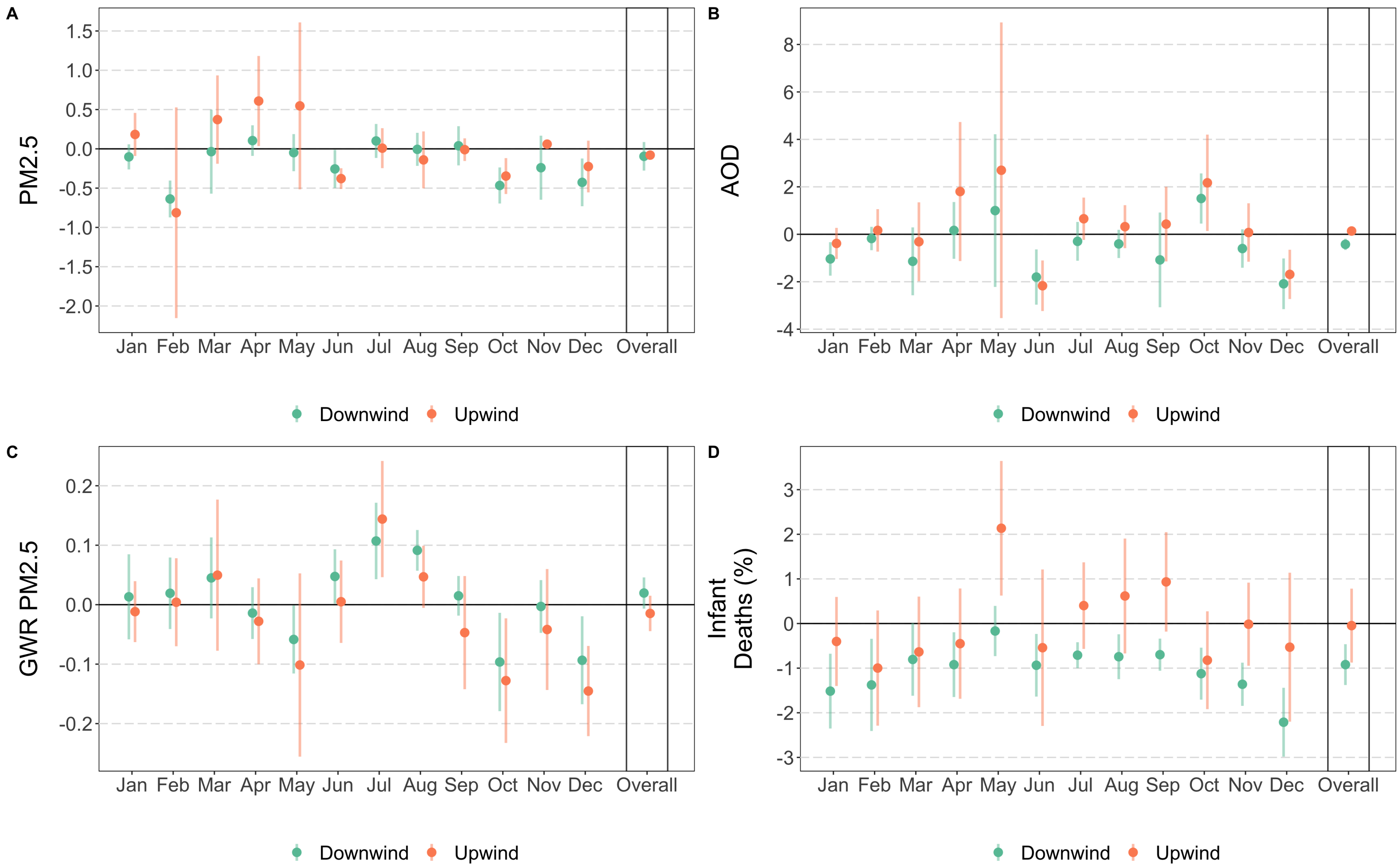


*Notes:* Coefficient estimates from equation (6) using BEM Area as the diffusion measure (all point estimates and confidence intervals are from one regression except for "Overall," which comes from equation (5)). Confidence intervals are calculated from Conley (1999) heteroskedasticity and autocorrelation robust standard errors with a uniform spatial kernel of 100 Km radius.

Figure A.5: Temporal Lags of Effects of Conservation Agriculture Exposure on Infant Mortality

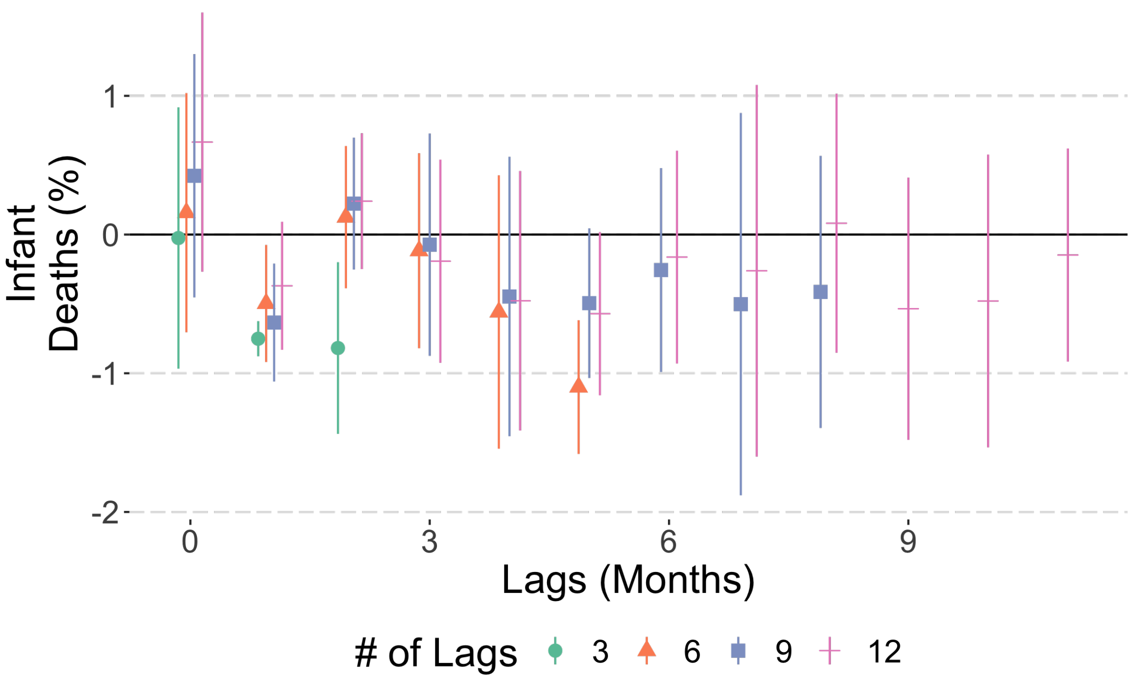

Figure A.6: Non-Agricultural Fire Event Study

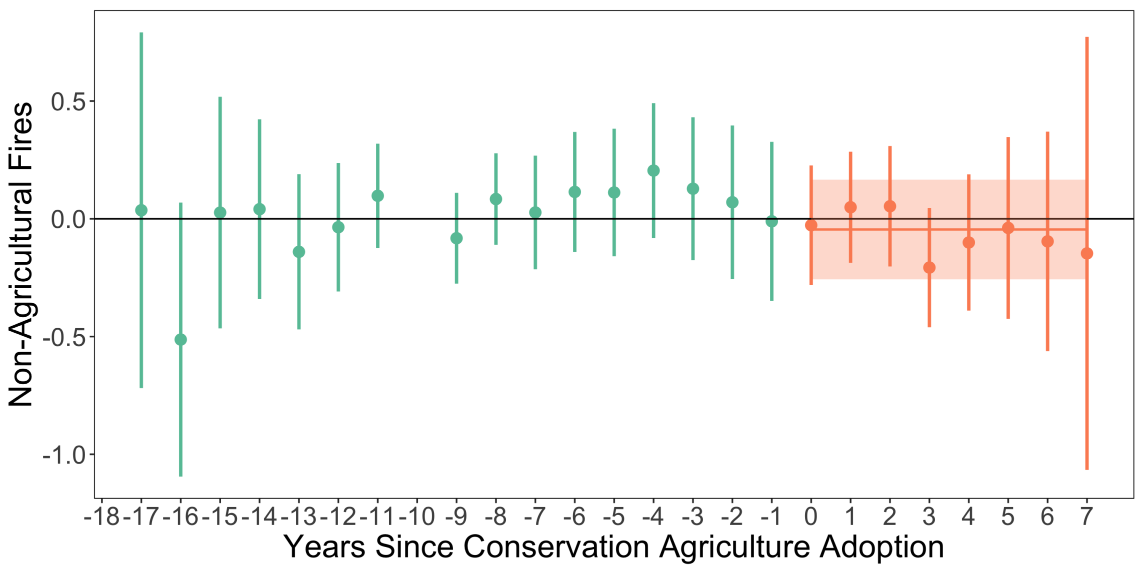


*Notes:* 95% confidence intervals for pre-treatment event time coefficients are constructed from standard errors clustered at the cell. 95% confidence intervals for post-treatment event time coefficients are constructed from conservative standard error estimates clustered at the cell level following Borusyak et al. (2021). The horizontal line across the post period is the difference-in-differences estimate and the shaded box is its 95% confidence interval constructed from conservative standard error estimates clustered at the cell level following Borusyak et al. (2021). The sample includes all cells that have a median number of agricultural fires per year greater than zero prior to 2012.

Figure A.7: Effects of Conservation Agriculture Adoption on Non-Agricultural Fires by Month

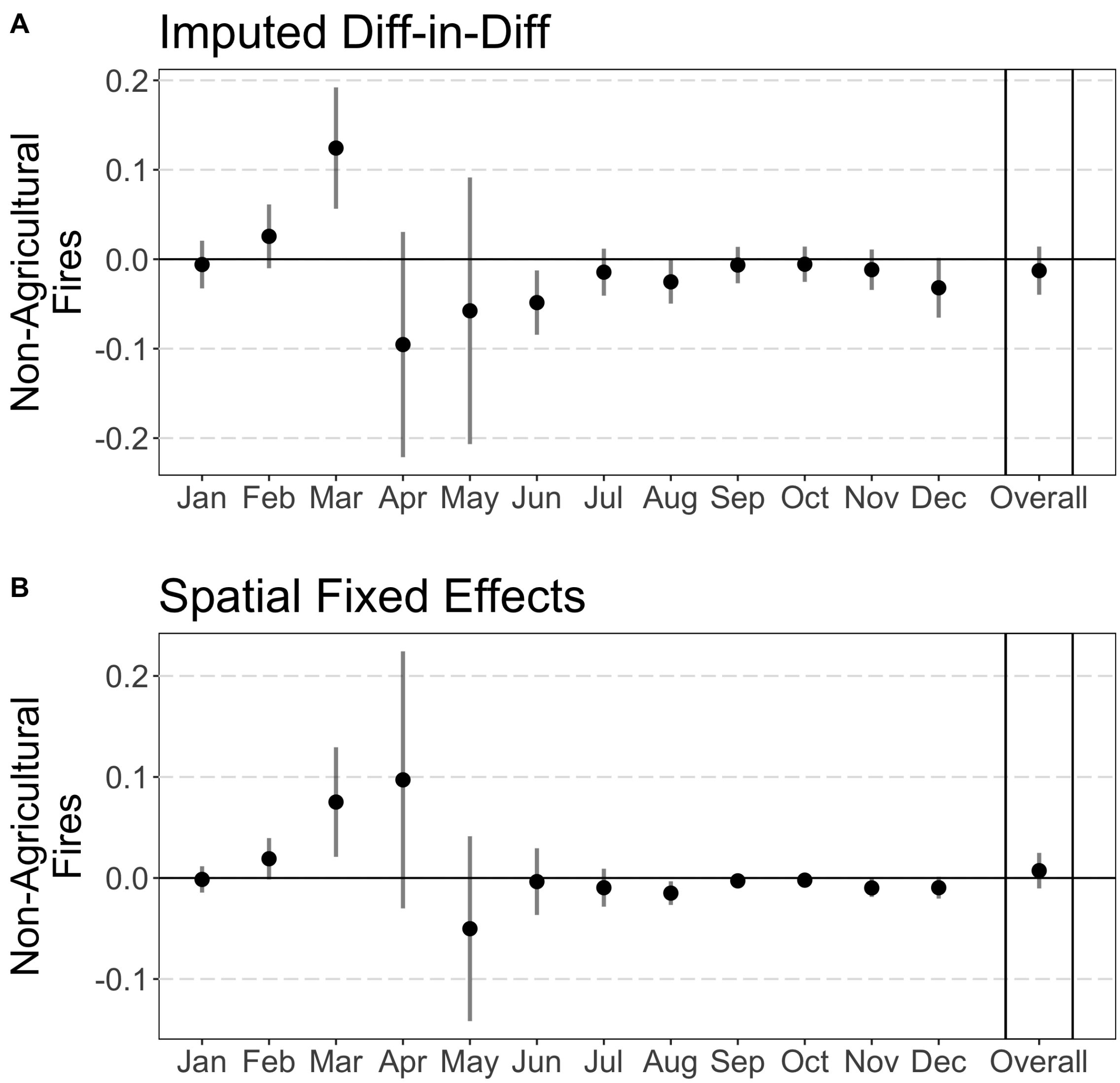


*Notes:* Coefficient estimates and 95% confidence intervals from equation 7 are shown in Panel A. Standard errors in Panel A are conservative estimates clustered at the cell level following Borusyak et al. (2021). The sample in Panel A includes all cells that have a median number of agricultural fires per year greater than zero prior to 2012. Coefficient estimates and 95% confidence intervals from equation 8 are shown in Panel B. Confidence intervals in Panel B are constructed using heteroskedasticity and autocorrelation robust standard error estimates with a 100km uniform spatial kernel following Conley (1999). The sample in Panel B is all cells have strictly positive agricultural land area according to the Soil Use Map Version IV.